Elevated Matrix Enzyme Activity Is Associated with the Progression of Pulmonary Vascular Disease In the Nitrofen Model of Congenital Diaphragmatic Hernia

This thesis is submitted to the Faculty of Graduate and Postdoctoral Studies in partial fulfillment of the requirements for the M.Sc. program in Cellular and Molecular Medicine

Benjamin Wild

The Faculty of Medicine
Department of Cellular and Molecular Medicine
University of Ottawa
Ottawa, Ontario, Canada

May, 2015

Abstract

Pulmonary vascular disease (PVD) and lung hypoplasia (LH) are the two main causes of mortality and morbidity in patients with congenital diaphragmatic hernia (CDH). Previous studies have shown that remodeling of the extracellular matrix (ECM) by elastase and matrix metalloproteinase (MMP) enzymes, concomitant with smooth muscle cell (SMC) proliferation and deposition of ECM proteins and growth factors, leads to primary pulmonary hypertension (PH) and that blockade of this pathway results in disease reversal. The aim of our study is to determine whether a similar pathway is induced in the PVD associated with CDH and to verify whether its inhibition will lead to reversal of PVD. Firstly, we confirmed various aspects of PVD in the nitrofen induced CDH rat model. These included: left lung hypoplasia, right ventricular hypertrophy, and increased arterial smooth muscle wall thickness alongside decreases in arterial lumen area and total number of distal pulmonary vessels. We also showed increases in elastase and matrix metalloproteinase (MMP) enzyme activities within distal pulmonary arteries (PAs), which, we were able to inhibit using serine elastase (sivelestat, elafin, and serpina1) and MMP (GM6001) inhibitors. Furthermore, we confirmed increased SMC proliferation and deposition of osteopontin (OPN) and epidermal growth factor (EGF) within the diseased vasculatures. We are now working on using sivelestat and GM6001 pharmaceuticals as well as endothelial progenitor cells (EPCs) and mesenchymal stem cells (MSCs) modified to express elafin and serpina1 to determine their abilities to reverse the PVD associated with CDH. This project is part of our translational research program with the ultimate goal of developing a novel strategy of targeting PVD in infants with CDH to improve patient survival and long-term outcome.

Table of Contents

List of Figures

List of Abbreviations

αβRAR$^{-/-}$ - α and β retinoic acid receptor knockout

AP – Alkaline Phosphatase

BPCA – 4-Biphenyl carboxylic acid

BMP – Bone morphogenic protein

BMPR – Bone morphogenic protein receptor

$[Ca^{+2}]_i$ – Internal calcium ion concentration

CDH – Congenital diaphragmatic hernia

CDH- – Nitrofen treated pups that did not develop CDH

CDH+ – Nitrofen treated pups that did develop CDH

Ctl – Olive oil treated pups

COUP-TFII$^{-/-}$ - Chicken ovalbumin upstream promoter transcription factor 2 knockout

E9/E12 – Embryonic day 9/12

EC – Endothelial cell

ECM – Extracellular matrix

ECMO – Extra-corporeal membrane oxygenation

EDTA – Ethylenediaminetetraacetic acid

EGF – Epidermal growth factor

EGTA – Ethylene glycol acetic acid

EMT – Endothelial-mesenchymal transition

eNOS – Endothelial nitric oxide synthase

EPC – Endothelial progenitor cell

ET – Endothelin

EXD – External diameter

FACS – Fluorescence activated cell sorting

FCS – Fetal calf serum

FGF – Fibroblast growth factor

FN – Fibronectin

GFP – Green fluorescent protein

HEK – Human embryonic kidney

HIF – Hypoxia inducible factor

HRP – Horseradish peroxidase

IP – Intraperitoneal

IT – Intratracheal

IV – Intravenous

K^+ - Potassium ion

LH – Lung hypoplasia

MMP – Matrix metalloproteinase

MSC – Mesenchymal stromal cell

MUC – Mucin

NHE – Sodium-hydrogen antiporter

NO – Nitric Oxide

OPN – Osteopontin

PA – Pulmonary artery

PAH – Pulmonary arterial hypertension

PASMC – Pulmonary artery smooth muscle cell

PBS – Phosphate buffered saline

PECAM – Platelet endothelial cell adhesion molecule

PEG-It – Polyethylene glycol solution

PCNA – Proliferating chain nuclear antigen

PH – Pulmonary hypertension

PPF – Pleuroperitoneal fold

PVD – Pulmonary vascular disease

PVDF – Polyvinylidenefluoride

P/S – Penicillin and streptomycin

RALDH-2 – Retinol dehydrogenase 2

RARE – Retinoic acid response element

ROCK – Rho associated protein kinase

RV/(LV+S) – Right ventricle divided by the sum of the left ventricle and septum

SDF – Stromal derived factor

$SLIT3^{-/-}$ - Slit 3 knockout

SMA – α-Smooth muscle actin

TNC – Tenascin-C

TSH – Thyroid stimulating hormone

VEGF – Vascular endothelial growth factor

$WT1^{-/-}$ - Wilm's Tumour knockout

µl - microliter

µg - microgram

µM – micromolar

ml - milliliter

mg - milligram

mM – millimolar

Acknowledgements

I would like to thank my supervisor Dr. Kyle Cowan as well as Dr. Stephanie Langlois for the opportunity to pursue this research and for providing me with the greatest possible chance at success. I was able to gain invaluable experience in performing a broad range of experiments and in presenting my research through there tutelage. Also, I would like to extend thanks to my thesis advisors; Dr. Duncan Stewart and Dr. Luc Sabourin for their continued guidance throughout the duration of my degree.

Furthermore, I would like to thank the following individuals for their assistance:
Xiao Xiang, Lynn Kelly and the rest of the staff at CHEORI for aiding in all the behind the scenes workings necessary for this project.

Introduction

1.1 Clinical data and significance of congenital diaphragmatic hernia

Congenital diaphragmatic hernia (CDH) is a condition whereby a developmental defect in the diaphragm allows for the invasion of abdominal viscerae into the thoracic cavity – a condition that causes detrimental effects to lung development. Interestingly, CDH is not well known outside the realm of neonatology even though it has a similar incidence as cystic fibrosis (Greer, Babiuk, and Thebaud 2003) at 1 in every 2500 births (Langham et al. 1996). CDH is associated with high mortality rates and morbidity and signifies the most life threatening condition causing respiratory failure in children due to the resulting lung hypoplasia (LH) and pulmonary hypertension (PH) (Thébaud, Mercier, and Dinh-Xuan 1998). Promising data suggests that mortality rates in highly equipped neonatal care centers, within the last decade, have dropped considerably from 50% to 20%, however, this increase in survival is met with an increase in treatment-related morbidity (Chiu et al. 2006; Downard et al. 2003). Altogether, the survival rates of CDH have reached 68%, although, this number is much lower when still births, therapeutic abortions and spontaneous abortions are included (Brownlee et al. 2009). Therefore, the need for a successful treatment strategy against the pathological vascular remodeling, defined hereafter as pulmonary vascular disease (PVD), associated with CDH is imperative to the survival and future well being of afflicted patients.

CDH can be broken down using a subclassification system based on hernia location and size. The Bochdalek hernia, as first characterized by Bochdalek in 1848, occurs most commonly in infants, represents 80% of all CDH cases, and is currently characterized as a posterolateral diaphragmatic defect whereby 85% are left-sided, 13% right-sided and 2% bilateral (Torfs et al. 1992). The Morgagni-type hernia, located anteriorly, tends to be much

smaller and has an occurrence of 17%. Finally, the transversum-type hernia is a centrally located hernia and occurs in 3% of all cases (Kays 2006; Rottier and Tibboel 2005). The cause of hernia laterality is still poorly understood.

The inherent morbidity associated with CDH is dependent upon CDH type. Altogether, morbidity can include gastrointestinal reflux, bronchopulmonary dysplasia, restrictive and obstructive lung disease, scoliosis, neurodevelopmental defects, neurosensorial deafness, and many more (Kotecha et al. 2012). Many of these secondary conditions are actually caused by the extreme treatment regiments required to treat patients with CDH, such as, chronic oxygen dependence, high frequency oscillatory ventilation, exogenous surfactant and nitric oxide (NO) administration, fetal tracheal occlusion, and extra-corporeal membrane oxygenation (ECMO) (Logan et al. 2007; The Neonatal Inhaled Nitric Oxide Study Group (NINOS) 1997). Unfortunately, unlike with many other conditions causing respiratory distress, many of these treatments have shown only limited success against CDH based mortality, with the exception of the highly invasive and still controversial ECMO technique. ECMO involves temporarily bypassing the lungs for a few days after birth to lower the blood pressure in the pulmonary circulatory system thereby relieving the vasculature from shear stress forces. This technique, however, is unable to reverse lung hypoplasia and imparts a heightened degree of morbidity in CDH patients (Bohn 2002).

Even though prenatal diagnosis has been possible for many years, CDH being easily observable by routine ultrasound around the 18-20 week mark of pregnancy, prenatal diagnosis and prognosis still cannot accurately depict the severity or survivability of the condition. This makes end of life decisions for parents difficult (Sokol et al. 2002). This difficulty is consistent with the fact that 50% of all CDH cases are only associated with LH and PH and the other 50% show additional abnormalities in the kidneys, heart, skeleton and

to neurogenesis (Costlow and Manson 1981; Greer, Babiuk, and Thebaud 2003). The causes of CDH, and the associated LH and PH conditions, remain unknown as only 5-10% of CDH cases are known to originate from chromosomal defects such as Denys-Drash Syndrome and trisomy 18 (Pober 2008). The ultimate goal in CDH research would be to elucidate a diaphragmatic defect causing mechanism followed by a treatment strategy targeting this mechanism in order to prevent the development of CDH entirely, or, to promote lung growth and inhibit the initiation or progression of PH in utero to increase patient survivability, decrease morbidity, and decrease the need for other invasive treatment methodologies.

1.2 Developmental physiology of the diaphragm, lung, and lung vasculature

To understand the diaphragmatic defect one must recognize the events of physiological diaphragm development. Unfortunately, the widely known series of events in the development of the diaphragm stems from a single publication (Wells 1954) dating back to 1954 when new age techniques such as transgenic animals and labeling techniques were unavailable. Even a recently published article (Keijzer 2010) details the finding from the 1954 paper and states that the musculature of the diaphragm originates from multiple sources, such as the septum transversum, esophageal mesentery, and the musculature of the posterolateral sides of the thoracic body wall (Keijzer 2010; Wells 1954). It has now been established, using a transgenic rat model, that the musculature of the diaphragm arises from cervical somites, whereby muscle precursors, alongside phrenic axons, migrate towards a primordial diaphragm designated as the pleuroperitoneal fold (PPF), expand, and differentiate. This event occurs around the 3-5 week mark of gestation in humans or embryonal day 12 (E12) to E13 in rats. By the 10th week of pregnancy in humans, or E17 in rats, when fetal breathing movements begin, muscle precursors are found positioned along

the underlying connective tissue and extend to the sternal, costal, and crural regions of the diaphragm surrounding the central tendon (Greer, Babiuk, and Thebaud 2003).

Since defects in pulmonary development are associated with CDH it is also important to know the developmental stages of the lung and lung vasculature. Lung development starts after cardiac morphogenesis has begun via cellular signaling between cardiac mesoderm and the endoderm of the foregut (Vincent and Buckingham 2010). Morphologically, the lungs begin as an outpouch of the ventral body wall of the posterior end of the laryngotracheal tube that then divides into 2 bronchial buds at the 3-4 week mark of pregnancy, or E10-11 in rats (Hopper and Hart 1985). The origins of the pulmonary vasculature are still unknown, however, it is believed to develop through both vasculogenesis and angiogenesis stimulated by uncharacterized pulmonary vascular precursors (Peng and Morrisey 2013). There are 4 distinct stages of lung development following the initialization stage. Undifferentiated primordial lungs and bronchial tree development are characteristics of the pseudoglandular stage whereas the initiation of terminal sac formation alongside vascularization occurs during the canalicular stage. The saccular stage is defined by large increases in terminal sac formation, vascularization, and differentiation of type I and II alveolar cells. The final stage, the alveolar stage, is characterized by a large expansion of alveoli and begins in utero in humans, postnatally in rats, and extends 7 years in humans, or 5 weeks in rats (Keijzer 2010).

1.3 Etiology of CDH

Due to the skewed view concerning the development of the diaphragm it was previously thought that CDH was caused by abnormal neuronal innervation, myotube expansion and differentiation, or fusion of the diaphragm with the lateral body wall, all hypotheses which remain unfounded. Instead it has been shown, again using rat models

causing CDH, that the pathogenesis of CDH can be traced back to the development of the PPF primordial diaphragm (Greer et al. 2005; Kluth et al. 1993) as defects in the PPF were shown prior to muscularization. This was again confirmed when tracking of muscle precursors to the PPF, as well as myotube expansion and differentiation, did not reveal any striking abnormalities even though a defective PPF was observable (Babiuk et al. 2002). The current hypothesis put forth to explain the etiology of CDH states that the amuscular substructure of the diaphragm, originating as the PPF, is defective and therefore cannot accommodate full diaphragmatic muscularization. Evidence that supports this hypothesis exists in the C-met null transgenic mouse model, whereby muscle precursors fail to migrate to form peripheral muscle. C-met is a tyrosine kinase receptor on muscle precursors that binds to hepatocyte growth factor and scatter factor to control migration (Bladt et al. 1995). The diaphragms of C-met null mice are therefore amuscular, however, the substratum originating as the PPF remains intact. Introducing various CDH causing teratogens into this transgenic model create defective PPFs and led to diaphragmatic hernias. Although this defect is associated with high mortality it may not be the main cause of CDH related mortality.

The two main causes of mortality in patients with CDH stem from LH and PH (Luong et al. 2011). Currently there are two main hypotheses linking the diaphragmatic hernia to PVD. Classically, it was thought that hypoplastic lungs were the result of lack of available thoracic volume, caused by invading abdominal viscera, and a reduction of mechanical strain, needed for proper lung development, caused by abnormal breathing motions (Cohen and Larson 2008; Wang et al. 2013). The more accepted viewpoint is coined the “two hit hypothesis”, whereby pulmonary development is disrupted due to both physical and developmental interferences. This is supported by data revealing defects to the retinoic

acid pathway, essential for organogenesis of many organs including the diaphragm and the lungs, in patients and animals with CDH (Malpel, Mendelsohn, and Cardoso 2000; Puri and Nakazawa 2009). Decreases in retinol levels have been observed during the period of diaphragm development in rats due to a transient increase in retinol utilization (Takahashi, Smith, and Goodman 1977). Notably, this time stage (E8-E12) corresponds to the pseudoglandular stage of development of the lungs (Hopper and Hart 1985), the developmental step known to be most affected by CDH (Cohen and Larson 2008). The lungs depend heavily on the retinoic acid pathway (Malpel, Mendelsohn, and Cardoso 2000) and defects in this pathway cause reduced airway branching, surfactant deficiencies, and vascularization deficiencies with extensive vascular muscularization. It is therefore thought that respiratory stress caused by CDH is due to both the physical impedance and developmental defects affecting the pulmonary system.

1.4 Teratogenic, genetic and surgical animal models for study of CDH

Animal models have played essential roles in determining the root cause of diaphragmatic defects alongside the effects of CDH on pulmonary development. They are also heavily relied upon for the development of novel surgical and therapeutic strategies against CDH as well as LH and PH caused by CDH. Fortunately, there are many animal models that can effectively create a CDH condition in fetuses. Animal models range from teratogenic in nature to genetic and even surgical. Surgical models have been employed in fetal lambs and involve implanting inflatable devices into the diaphragm to create a CDH-like defect (Aubry et al. 2013). This model was essential for the discovery of the tracheal occlusion and surfactant administration treatments found to be partially successful in

lowering CDH related mortality, however, could not correctly mimic the "two-hit hypothesis" most accepted by the CDH community (Dekoninck et al. 2011).

Genetic animal models come from transgenic mouse models for various gene knockouts. The first genetic CDH model was founded when a slit3 knockout ($SLIT3^{-/-}$) was established (W. Yuan et al. 2003). Slit proteins are required for axonal guidance, extension, and growth, and therefore improper axonal innervation of the diaphragm, due to slit knockout, is the expected mode of action in creating the rare centrally located transversum-type hernia. Other models include Wilm's Tumour 1 ($WT1^{-/-}$) and chicken ovalbumin upstream promoter transcription factor II ($COUP\text{-}TFII^{-/-}$) knockouts, both of which effectively create the more common left sided Bochdalek hernia (Moore et al. 1998, 1999).

Teratogenic animal models of CDH are by far the most common models used to study diaphragmatic defects and respiratory disease also present in infants with CDH. 4-biphenyl carboxylic acid (BPCA), a thromboxane-A_2 receptor agonist, bisdiamine, a spermatogenesis inhibitor, SB-210661, a benzofuranyl urea derivative that inhibits S-lipoxygenase, and nitrofen, a now banned herbicide are all teratogens that cause CDH with similar secondary characteristics to the human condition when given between E9-E11 in mice and rats. The nitrofen induced CDH rat model is the most used model in the CDH community (Greer 2013). Nitrofen (2,4-dichloro-1-(4-nitrophenoxy) benzene) is a protox inhibiting herbicide of the biphenyl ether class. Nitrofen is currently banned in developed nations for carcinogenic effects on rodents and is classified as a group 2B carcinogen (Lunn 2011). Toxicology reports found that rat pups exposed to nitrofen in utero appeared cyanotic, showed signs of respiratory distress, presented with CDH, and died shortly after birth (Manson 1986). Feeding pregnant rats orally with 100mg of nitrofen between E8 and E12 (4-6 weeks in humans) produced hypoplastic lungs and CDH in 50% of pups (Stone and

Manson 1981). The nitrofen exposed pups not exhibiting CDH, however, did show kidney, heart, and skeletal defects (Costlow and Manson 1981; Greer, Babiuk, and Thebaud 2003). Historically, it was thought that nitrofen acted as a thyromimetic, due to its structural similarity to thyroid hormone, to disrupt the maternal-fetal thyroid hormone pathway by suppressing maternal thyroid stimulating hormone (TSH) levels (Manson 1986). Conversely, nitrofen has been shown to be delivered directly to pups rather than exerting its effects via maternally produced active metabolites (Brown and Manson 1988). Therefore, an alternative mechanism may likely be a root cause of the diaphragmatic defects. Whatever the mechanism of action, nitrofen has been shown to produce many structural abnormalities seen in the human CDH condition, such as, relative diaphragmatic defect size and location, LH, pulmonary artery medial wall thickening and right ventricular hypertrophy (Clugston et al. 2006).

1.5 Developmental dependence of the diaphragm and lung on the retinoic acid pathway

One hypothesis put forth to explain the effect of these animal models on diaphragm organogenesis is an altered retinoic acid pathway. This hypothesis was formulated when studies determining the effect of vitamin A deficiencies were conducted on rodents. These studies found that 25-40% of offspring presented with CDH with the majority of cases being right sided defects (Anderson 1941, 1949). CDH occurrence was then notably diminished when vitamin A was introduced during mid gestation (Wilson, Roth, and Warkany 1953).

Since vitamin A was shown to be crucial for the organogenesis of the diaphragm, it was theorized that all CDH causing teratogens were creating similar phenotypes by inhibiting the retinoic acid pathway, in particular, by inhibiting retinal dehydrogenase 2

(RALDH-2). To test this, an immortalized oligodendrocyte cell line (OLN93) was used as a source of dehydrogenase. These cells were cultured with each of the teratogens capable of inducing CDH and tested for their ability to synthesize retinoic acid from all trans retinal (Mey et al. 2003). All teratogens effectively inhibited RALDH-2 with bisdiamine being the most potent inhibitor – also known to cause CDH with the highest prevalence of any teratogenic CDH animal model. Interestingly, co-administration of vitamin A with these teratogens in vivo decreased CDH prevalence by 15-30% and attenuated LH (Thébaud et al. 2001; Thébaud et al. 1999).

This pathway, although not yet confirmed to be a factor in the human CDH condition, is supported by findings showing that in 50% of newborns with CDH present with retinol and retinol binding protein plasma level deficiencies (Major et al. 1998). One limitation of this study, however, was the small sample size. A larger study is thus needed to confirm these results. Chromosomal defects in areas known to encode proteins essential to the retinoic acid pathway have also been shown to be present in 10% of human CDH cases (Enns et al. 1998). Due to the large percentage of CDH cases where retinol levels are not shown to be significantly altered compared to normal levels, the etiology of CDH remains unconfirmed. New data, however, using the nitrofen CDH rat model suggests that another cause for decreased retinol levels during fetal development is decreased levels of retinol binding protein expression within the placenta (Kutasy et al. 2014). This leads to defects in the transport of retinol from the placenta to the fetus, an accumulation of retinyl-ester in the placenta and lower than normal levels of retinol in the fetus. Studies on retinol or retinol binding protein levels have only been performed on newborn blood samples and not on placental or fetal specimens. Performing these tests on fetal blood may provide evidence that defective retinoic acid signaling is indeed the major cause of CDH in humans.

1.6 Pulmonary hypertension

As previously mentioned, the major causes of mortality in patients with CDH are LH and PH (Luong et al. 2011). It is still unknown whether PH forms due to LH or vice versa, however, it has been shown that successfully treating one will produce beneficial effects on the other (Luong et al. 2011). Because PH has been studied extensively, mostly in non-CDH environments, with promising results and because treatments against LH have been relatively unsuccessful, treating PH in patients with CDH may be a more realistic approach to increasing the overall survival of patients with CDH.

PH can be classified into 5 somewhat distinct categories according to diagnosis (Simonneau et al. 2004), however, is simply defined as pulmonary arterial (PA) pressure above 25mmHg at rest or 30mmHg. Category 1 encompasses pulmonary arterial hypertension (PAH) and includes idiopathic, familial, and acquired PAH. Acquired PAH is associated with collagen vascular disease, portal hypertension, various drugs, HIV, and various other conditions. PH in newborns has also been classified under category 1. Categories 2-5 include PH caused by left sided heart disease/myocardial dysfunction, lung disease/hypoxemia, chronic thrombotic/embolic disease, and miscellaneous disorders respectively.

In newborns with CDH or other conditions that cause PVD, PH develops from the inability of the pulmonary vasculature to compensate for the increased ventricular output once the ductus arteriosus and foramen ovale close at birth (Rudolph 1970). Under physiological conditions, the vasculature dilates and undergoes remodeling resulting in the apoptosis of pulmonary arterial smooth muscle cells (PASMCs) to allow for proper gas exchange during respiration (Rabinovitch 2008). Under pathological conditions such as PH,

the vasculature is unable to dilate thereby promoting inflammatory responses, abnormal muscularization of distal PAs and an overall decrease in the number of distal vessels. Muscularization of distal vessels is mainly due to the differentiation of pericytes to PASMCs that then proliferate (Meyrick and Reid 1980). It has also been shown that PASMCs in distal vessels can even originate as endothelial progenitor cells (EPCs). Many current treatment strategies have been focused around reducing abnormal vascular remodeling induced by PH by stimulating apoptosis in abnormal PASMCs and promoting regeneration of lost distal vasculature (Rabinovitch 2008).

1.7 Vascular remodeling

Evidence supporting vascular remodeling in humans was discovered when post mortem analysis of children living in high altitude environments found muscularized distal arterioles. Also, adults from these same regions were diagnosed with increased pulmonary vascular resistance and right ventricular hypertrophy (Penaloza et al. 1964; Rotta et al. 1956). This led to the discovery of the chronic hypoxia model for PH. Rats living in hypoxic conditions have been found to show right ventricular hypertrophy, increases in arterial smooth muscle wall thicknesses, distal vessel muscularization, outward growth of PASMCs and incomplete vasodilation (Berg 2007; Stenmark et al. 2009), however, do not present with any loss of distal vasculature as shown in PAH. One dose of SU5416, a vascular endothelial growth factor (VEGF) inhibitor followed by hypoxia did however cause endothelial cell (EC) apoptosis followed by a resurgence of apoptosis-resistant ECs and led to vascular occlusion and loss of distal vessels (Taraseviciene-Stewart et al. 2001). Other animal models of primary PH include monocrotaline administration causing inflammation and EC injury,

serotonin administration, bone morphogenic protein receptor 2 knockouts, and all models causing CDH.

It is now widely accepted that defects within the vasculature contribute to all forms of PH. These defects include but are not limited to; stiffening of the proximal arteries, thickening of the intimal and medial layers of arteries and arterioles (Tuder 2009), vaso-occlusive lesions caused by either PASMC or EC proliferation and migration, and the appearance of cells expressing SMC markers in normally non-muscular vessels (Voelkel and Tuder 2000). The hallmarks of all forms of PH include vasoconstriction/incomplete dilatation and vascular remodeling. More recently it has been shown that endothelial-mesenchymal transdifferentiation of ECs may also play an important role in the development of PH (Stenmark et al. 2009). The main effector of the changes in vascular resistance with all forms of PH stems from pathogenic remodeling of small distal arterioles whereas decreased compliance of large proximal arteries, although the main driving force behind development of right ventricular hypertrophy, only contributes a small portion to increases in vascular resistance (Gan et al. 2007; Mahapatra et al. 2006). Historically, vascular remodeling was thought to occur via the inward movement of cells causing vascular occlusion leading to increased vascular resistance, heart defects, and eventual death as seen in PAH. Now it is thought that the outward growth of cells combined with decreased luminal areas, due to incomplete vasodilation, are features that cover a broader scope of vascular remodeling and are consistent features in multiple forms of PH (Stenmark and McMurtry 2005) and not just PAH.

1.8 Elastase and MMP enzymes

The extra cellular matrix (ECM) is a dynamic, constantly changing system that creates highly specialized cellular environments that affect cell development, differentiation, morphogenesis, adhesion and many more cellular properties (Visse and Nagase 2003). It has been previously shown that vascular remodeling is caused by changes in the composition of the ECM (Cowan et al. 2000). Proteases are enzymes that perform proteolysis. Proteolysis represents a catabolic reaction for protein degradation resulting from hydrolysis of peptide bonds that form a protein and has been found to be the main driving force behind changes to ECM composition and therefore, cellular environments (Woessner 2004). Proteases can be classified based on both target proteins and by method of proteolysis. Serine proteases utilize a serine amino acid residue in their catalytic site to perform hydrolysis whereas cysteine, aspartate and metalloproteases use cysteine thiol residues, carboxylic acid residues, or a metal ion, most commonly zinc, respectively (Woessner 2004). Of particular interest to pulmonary vascular remodeling are elastase and matrix metalloproteinase (MMP) enzymes.

Elastase enzymes are specific proteases essential for the break down of elastin, an essential building block of connective tissue and a key structure within the pulmonary vascular system. Elastase enzymes also have the immunological role of breaking down proteins on the outer membrane of Gram negative bacteria (Horwitz et al. 1999). Like most proteases, elastase enzymes can be distinguished based on their method of elastin degradation; as serine elastase, cysteine elastase and metalloelastase. It has been established that rampant elastase activity due to the loss of serpina1, a serine protease inhibitor expression, results in pulmonary emphysema (Horwitz et al. 1999). As previously mentioned, serine elastase inhibition led to the complete regression of monocrotaline induced primary PH by reversing the effects of vascular remodeling (Cowan et al. 2000).

MMPs are proteases responsible for degrading various ECM components via a zinc binding domain (Nagase and Woessner 1999). Loss of control of MMP activity through elevated protein expression, elevated activation, or loss of tissue inhibitors of MMPs (TIMPs), is associated with cancer, atherosclerosis, ulcers and other severe conditions (Woessner 1998). MMPs have been classified into 6 groups based on their substrates. Collagenases, such as MMP1, 8, 13, and 18 cleave collagens I, II, III and other ECM molecules (Visse and Nagase 2003), gelatinases, such as MMP2 and 9 digest denatured collagen, laminin and gelatins (Allan et al. 1995), stroelysis, matrilysins, membrane-type MMPs, and others, process cell surface molecules, digest ECM components and are essential for macrophage migration (Ohuchi et al. 1997; Shipley et al. 1996). MMP2 and 9 in particular, representing the gelatinase class of MMPs, have both been shown to play crucial roles in the development and maintenance of PH (Cowan, Jones, and Rabinovitch 1999).

1.9 Induced matrix enzyme activity and proteolytic degradation of ECM proteins causes vascular remodeling

Recently, it has been discovered that vascular remodeling due to induced proteolytic activity and degradation of ECM proteins surrounding PASMCs is seen in most conditions involving PH (Cowan et al. 2000). As previously mentioned, the hallmarks of progressive PH are increased cell proliferation and migration from the medial to the neointimal layers of PAs. It has been shown that growth factor dependent proliferation and migration depend on ECM proteins tenascin-C (TNC) and fibronectin (FN) respectively as exogenously added TNC to cultured rat PASMCs on collagen-type 1 increased the mitogenic effects of fibroblast growth factor 2 (FGF-2) and was a prerequisite for epidermal growth factor (EGF) dependent proliferation (Jones and Rabinovitch 1997). TNC is an ECM $\alpha_v\beta_3$ integrin binding protein

expressed during tissue restructuring in a variety of tissues such as the brain and lungs and mediates cell proliferation and expression of genes in a tissue specific manner (Bartsch et al. 1992; Jones et al. 1995; Whitby and Ferguson 1991). FN is also an ECM glycoprotein expressed during embryonic development and wound healing and is known to play roles in cell adhesion, growth, migration and differentiation (Pankov and Yamada 2002).

In advancing forms of PH and other PVDs, TNC expression is highly upregulated in the neointimal layers of PAs and co-localizes with EGF whereas FN accumulates in the periendothelium (Botney et al. 1992). Interestingly, MMP enzymes, responsible for proteolytic cleavage of TNC and FN, have also been shown to stimulate the secretion of TNC and FN (Todorovich-Hunter et al. 1988). It was found, using experimental models involving rats and calves, that increased ECM deposition of FN, TNC, thrombospondin, type-1 collagen, elastin, as well as an induction of ECM degrading enzymes, such as MMPs and elastases, was responsible for the production and release of a variety of PASMC bound mitogens, such as the previously mentioned FGF-2, which all stimulated vascular remodeling (Botney et al. 1992).

Cultured PAs from rats treated with monocrotaline to induce primary PH were found to overexpress TNC and FN when compared to controls (Jones, Crack, and Rabinovitch 1997). Treating these PAs with antisense TNC RNA, to eliminate TNC translation, successfully inhibited TNC dependent proliferation however only stopped the progression and did not reverse the existing hypertrophy (Cowan, Jones, and Rabinovitch 2000). Osteopontin (OPN), a similar $\alpha_v\beta_3$ integrin binding ECM protein to TNC, usually expressed during bone remodeling and immune responses, was found to compensate for the lack of TNC and was able to maintain hypertrophy (Cowan, Jones, and Rabinovitch 2000). Again using organ cultures of PAs, this time comparing cultured porcine PAs in attached versus

floating collagen gels, it was found that PAs in attached gels had elevated levels of MMP activity, which led to an upregulation of TNC, and therefore increased PASMC proliferation whereas the opposite was found on floating gels (Cowan, Jones, and Rabinovitch 1999). This culture system was used to determine the effects of cell shape and integrin binding on progression of hypertrophy. Repeating this experiment using rat PAs provided an amplified response where MMP2, MMP9, elastase, as well as elastin deposition was also associated with medial wall thickening of PAs attached to collagen gels (Cowan, Jones, and Rabinovitch 1999).

The medial wall thickening observed in PAs cultured on attached gels was successfully inhibited using GM6001, a potent MMP inhibitor (S. Merklinger et al. 2005). GM6001 was also able to reverse the hypertrophy seen in explant PAs from rats treated with monocrotaline. Exogenous addition of TNC to GM6001 treated PAs then recreated the hypertrophied phenotype. ZD0892, a serine elastase inhibitor, was also able to regress the hypertrophy seen in cultured PAs to an even higher degree than GM6001 (Cowan, Jones, and Rabinovitch 2000). It was then hypothesized that elastase and GM6001 inhibitors could reduce the effects of PH in vivo. Twenty one days after a monocrotaline injection, when experimental primary PH had fully developed in adult rats, rats were treated with either ZD0892 or M249314, both serine elastase inhibitors (Cowan et al. 2000). After 1 week, 92% of monocrotaline-injected rats treated with a serine elastase inhibitor survived compared to the 39% of vehicle treated controls. After 2 weeks, 86% of treated rats survived whereas 0% of vehicle treated rats remained. These survival values alongside measured decreases in right ventricular hypertrophy, mean pulmonary arterial pressure, medial wall thicknesses, TNC accumulation, ECM deposition (such as elastin), and cell proliferation alongside increases in

PASMC apoptosis confirmed a complete reversal of monocrotaline induced primary PH (Cowan et al. 2000).

1.10 Alterations in ROCK, BMPR2, endothelin-1 and HIF signaling also causes vascular remodeling

In addition to proteolytic degradation, Rho kinase and the ROCK pathway have recently been shown to be affected in many cases of PH. ROCK signaling plays a key role in vasoconstriction as seen in all types of PH (Oka et al. 2007). RhoA and RhoB, upstream activators of ROCK, upon activation, led to cytoskeletal rearrangements in PASMCs and ECs with RhoB also positively affecting migration and proliferation under hypoxic conditions (Martin et al. 2012; Oka et al. 2007). ROCK inhibitors have successfully been shown to decrease pulmonary vascular resistance and PA pressure, however, also caused systemic hypotension when given via intraperitoneal (IP) injection. Inhaled ROCK inhibitors, on the other hand, localized to the lungs and did not cause systemic hypotension in rats (Nagaoka et al. 2005). Of note, sildenafil and statins have been found to inhibit ROCK signaling however the extent of which is unknown (Guilluy et al. 2005).

Bone morphogenic protein (BMP) signaling defects have also been shown to be critical for many types of PAH. BMPs bind to type I or II BMP receptors resulting in SMAD dependent and independent signaling pathways which culminate in the nuclear translocation of various transcription factors (Lowery and de Caestecker 2010). BMP signaling also affects MAP kinase, phospholinositol 3-kinase/AKT, and protein kinase C pathways (X. Yang et al. 2007) in up to 50-60% of all human CDH cases (Gosemann et al. 2013). Interestingly, BMPs have differential effects on PASMCs depending on location within the pulmonary vasculature. BMP2+4 are antiproliferative in proximal PASMCs but increase proliferation in

distal PASMCs (X. Yang et al. 2005). BMPR2 mutations have been well characterized in PAH and hypoxic animal models and have been shown to lead to the loss of the antiproliferative effect of BMP2 (Davies and Morrell 2008). In ECs, loss of BMPR2 leads to apoptosis whereas activation by BMP2+4 leads to production of NO (Gangopahyay et al. 2011). Sildenafil has been used to restore BMP signaling in PASMCs associated with PH (J. Yang et al. 2013) although has not shown sufficiently beneficial effects to be used globally in humans (Luong et al. 2011).

As previously mentioned, incomplete vasodilation is seen in all forms of PH. One reason is due to higher than normal levels of endothelin, a potent secretory vasoconstrictor peptide (Yanagisawa et al. 1988). There are 3 forms of endothelin with endothelin-1 (ET-1) having the highest endogenous expression levels. ET-1 has been shown to cause vasoconstriction alongside increases in migration and proliferation of vascular cells (Shao, Park, and Wort 2011). ET-1 binds to ET_A and ET_B membrane receptors and results in inhibition of K^+ channels, increased cellular calcium concentrations ($[Ca^{+2}]_i$), and activation of ROCK signaling (Shimoda et al. 2002; Undem et al. 2012; Whitman et al. 2008). ET_A, found in PASMCs, activation specifically results in contraction, proliferation and migration whereas ET_B, absent in PASMCs but present in ECs, acts like an ET-1 sink. Interestingly, circulating ET-1 levels are elevated in all animal models and human forms of PH (Shimoda et al. 2002). ET receptor inhibitors have been tested and were successfully able to improve exercise capacity and survival through an unknown mode of action (Davie et al. 2009).

Another vascular remodeling agent, termed hypoxia-inducible factor (HIF), is also known to promote the development of PH. HIF-1 is an oxygen sensitive transcription factor and exists in two forms: α, only expressed under hypoxic conditions and β which is constitutively expressed. HIF-1α degradation is mediated by hydroxylation from 2 proline

residues using molecular oxygen as a substrate followed by binding of von Hippel-Lindau protein, ubiquitination and proteasomal degradation (Semenza 2005). Decreased molecular oxygen limits HIF-1α hydroxylation and therefore degradation and allows HIF-1α to activate various transcription factors leading to cell proliferation. The mechanism is still under investigation however speculation links HIF-1α to $[Ca^{+2}]_i$ and pH homeostasis (Shimoda 2010).

1.11 Capability of EPCs and MSCs to home to hypoxic sites and induce cellular repair

Current treatments for CDH in humans involve post-natal administration of therapeutics such as NO, sildenafil, O_2, and others (Kinsella, Ivy, and Abman 2005), however, there is an ever-increasing bank of evidence showing the efficacy of using stem cells to promote organ repair (Bussolati 2011). Currently, the cells most frequently used to promote lung regeneration and vascular repair are endothelial progenitor cells (EPCs) and mesenchymal stromal cells (MSCs). These cells are found in abundance in the umbilical cord and cord blood and can easily be expanded and enhanced ex vivo before being re-administered to the patient (Fung and Thébaud 2014). In utero stem cell treatment is also possible as potent stem cells may be extracted from placental fluid, although this treatment would be inherently more risky.

EPCs can differentiate from bone marrow or umbilical cord hematopoietic cells and can circulate throughout the circulatory system (Shi et al. 1998). They have been shown to promote angiogenesis and home to hypoxic tissue to promote vascular repair and have even been shown to transform into mesenchymal cells through the well-characterized endothelial-mesenchymal transition (EMT) (Lamouille, Xu, and Derynck 2014). There are 3 stages

during EPC homing to sites in need of repair: 1) adhesion to ECs, 2) incorporation into capillaries, and 3) transendothelial migration to extravascular spaces (Hur et al. 2007). Mouse hind limb ischemia models have shown that transplanted EPCs migrate preferentially to the hypoxic ischemic hind limb and effectively stimulate angiogenesis (Hur et al. 2007; Yamahara et al. 2008; Yan et al. 2009), both representing desirable effects for a treatment against PH. The number of native EPCs in target organs may be a limiting factor in the therapeutic effect of angiogenesis stimulating therapies, therefore, administering ex-vivo expanded cells may increase homing and vascular formation in hypoxic tissue (Rafii and Lyden 2003). The mechanism for EPC trafficking is still under investigation however it is known that tissue expressing elevated amounts of VEGF and stromal-derived factor 1 (SDF-1) are target sites for EPC trafficking (Kawamoto et al. 2004; Yamaguchi et al. 2003).

EPCs have already been used as vesicles to deliver an endothelial nitric oxide synthase enzyme (eNOS) in a primary PH model (Zhao et al. 2005). Although EPC engraftment was not noticeable, around 5% in the lungs, a complete reversal of PH was attained. Transplanted EPCs without the eNOS gene were also shown to stop the progression of PH however could not reverse the existing hypertrophy (Zhao et al. 2005). It may therefore be possible that EPCs modified to express elafin or serpina1, serine elastase and serine protease inhibitors respectively, will home to sites of injury within the pulmonary vasculature, reverse the effects of PH secondary to CDH, and initiate angiogenesis to regrow vessels lost due to the progression of PH.

MSCs, also derived from bone marrow and umbilical cord tissue, have been used to promote organogenesis, tissue regeneration, maintenance, and repair in a variety of settings such as in cardiovascular and neurodegenerative disorders (Weiss et al. 2011). MSCs represent a viable source of stem cells due to their ease of isolation, characterization,

multipotency, and pleiotropic effects. It has also been shown that MSCs can home to injured lungs, differentiate into alveolar epithelia, promote lung repair, and prevented lung injury (Griffiths, Bonnet, and Janes 2005; Weiss et al. 2011). Umbilical cord derived MSCs have been used in a hyperoxia animal model, which induced lung injury and inflammatory responses, and were able to improve alveolar growth in a dose dependent manner whereby a dose of $5x10^5$ cells via IP or intratracheal (IT) injection attenuated lung injury (Chang et al. 2009). The mechanisms for MSC homing and repair are only now being explored however to date it is known that MSCs induce cellular repair via paracrine signaling by membrane vesicles, exosomes and nanopackages with bioactive molecules, and microRNAs (Chaput and Théry 2011). This was verified when MSC conditioned media, administered intraventricularly (IV), normalized lung function, reversed alveolar injury, and attenuated PH in a hyperoxia animal model (Hansmann et al. 2012). The therapeutic effects from MSC conditioned media were then enhanced when MSCs were primed under hyperoxic conditions (Waszak et al. 2012). The MSC paracrine effect has been shown to have the ability to modulate the function of inflammatory cells, increase the number of bronchoalveolar stem cells, and direct macrophages from the proinflammatory M1 phase to a healer M2 phase in a variety of disease conditions (Ionescu et al. 2012; Kim et al. 2005; Tropea et al. 2012). MSC derived exosomes have also been shown to prevent vascular remodeling (Lee et al. 2012). Clinical trials, currently underway to determine the safety of MSC transplantation in an obstructive pulmonary disease setting, have shown promising safety results, however, in this study, efficacy was not recorded (Weiss et al. 2013). For all of theses reasons it is apparent that enhanced MSCs have the potential to both reverse the effects of PH and stimulate lung growth and repair in hypoplastic lungs and therefore, could be a prime candidates for use as a treatment in patients with CDH.

1.12 Hypothesis and objectives

Due to the convincing data showing complete regression of primary PH in the monocrotaline model and knowing one of the main causes of mortality in infants with CDH is the associated PH, we hypothesize that an elevation in matrix enzyme activity is associated with the progression of PVD associated with nitrofen-induced CDH in fetal rats. Inhibition of this activity may mediate disease reversal, improve survivability, and decrease morbidity in patients with CDH. To test this hypothesis we determined whether the upregulation of matrix enzyme activity and downstream molecular pathway previously identified in the progression of primary PH is consistent with the progression of PH secondary to CDH, characterized the matrix enzyme activity for future inhibitor treatments, and will be assessing whether inhibition of the CDH-induced matrix enzyme activity in vivo, with sivelestat, GM6001, and EPCS/MSCs expressing elafin or serpina1, will led to disease reversal and increase survival.

Materials and Methods

2.1 Nitrofen induced congenital diaphragmatic hernia rat model

All procedures and protocols (protocol numbers: CHEO-105 and CHEO-106) were submitted and approved by the Animal Care Committee at the University of Ottawa, Ottawa, Ontario, Canada.

To produce a left-sided CDH, timed-pregnant Sprague-Dawley rats were gavage fed with 100 mg of nitrofen (Sigma, 33374) dissolved in 1mL of olive oil on E9, as previously described (Noble et al. 2007). Control animals received 1mL of olive oil only. The pups were harvested at term (E21) via caesarean section after the mothers were euthanized with an intraperitoneal (IP) injection of a lethal dose of Euthanyl Forte (provided by the Animal Care Committee at the University of Ottawa). Fetuses were weighed and decapitated for evaluation of the presence of CDH. Lungs and hearts were harvested and the left lungs weighed independently. Left lungs were analyzed because the nitrofen CDH rat model produces left sided diaphragmatic defects thereby affecting left lung development to the greatest degree. Since not all fetuses exposed to nitrofen presented with CDH, fetal rats were divided into three groups: fetuses exposed to olive oil (Ctl), fetuses exposed to nitrofen but did not develop CDH (CDH-), and fetuses that were exposed to nitrofen and developed CDH (CDH+).

2.2 Right ventricular hypertrophy

Once the hearts were dissected from the fetal rats the atrial chambers were removed and the right ventricle (RV) was dissected from the left ventricle plus the septum (LV+S), and weighed separately. As an index of right ventricular hypertrophy, the weight ratio (RV/LV+S) was then calculated (Cowan et al. 2000).

2.3 Lung to body weight ratio

Left lungs were used to establish the lung to body weight ratio, an indicator of LH (Luong et al. 2011).

2.4 Preparing whole lung lysates

Four CDH+, CDH- and control fetal rat lungs previously flash frozen in liquid nitrogen and stored at -80^{o}C were placed in 1ml of lysis buffer containing 1% Triton X-100, 150mM NaCl, 10mM Tris, 1mM EDTA, 1mM EGTA, 0.5% NP-40 and 0.05% PhosStop (Roche, 4906845001) and homogenized using a polytron homogenizer (Brinkmann, PT10-35). The resulting mixture was kept on ice, vortexed every 5 minutes for 30 minutes and centrifuged at 12,000rpm at 4^{o}C for 10 minutes to remove cellular debris. Lysates were then assessed via western blotting.

2.5 Western blotting

Cells to be analyzed were lysed using the aforementioned lysis buffer, washed with PBS, and centrifuged at 12,000rpm for 10 minutes. The supernatant was then collected and stored at -80^{o}C. Gels were cast and protein was transferred onto PVDF membranes (Bio-Rad, 170-4157) using the Transblot Turbo transfer system (Bio-Rad, Berkeley, California). PVDF membranes were stained with antibodies for PCNA (1:1000, Abcam, 2428), active caspase-3 (1:500, Abcam, 13847), EGF (1:500, Novus Biologicals, NBP1-19806), OPN (1:1000, Abcam, 8448), TNC (1:1000, Abcam, 108930), α smooth muscle actin (SMA) (1:200, Abcam, 134813), MMP2 (1:200, Novus Biologicals, NB200-193), elafin (1:200, Santa Cruz, sc-20637), serpina1 (1:500, Origene, TA500371), PECAM-1 (1:200, Santa Cruz, sc-28188), MUC1 (1:200, Abcam, ab45167), tubulin (1:1000, Santa Cruz, sc-8035) or myc (1:1000, Millipore, 05-724) and proteins were detected using either a goat anti-rabbit Alexa Fluor 680

(Invitrogen, 1027681) or an anti-mouse IRDye800 (Li-Cor, IRDye800CW) secondary. The PVDF membranes were then scanned on an Odyssey CLx western blot scanner (Li-Cor, 9140-01).

2.6 Immunohistochemistry

Left lungs from control, CDH-, and CDH+ fetal rats were fixed in 4% paraformaldehyde for 48 hours and processed for histology. Left lungs were embedded in a 21-tissue microarray (7 left lungs from each treatment group) with the hilum in the sectioning plane, and sectioned to a 4µm thickness. The use of tissue microarrays allowed for all samples to be processed on one slide, which allowed for direct comparison of immunohistochemical staining between tissue samples. The microarrays were stained with mouse antibodies against PCNA (1:1000), active caspase-3 (1:100), and anti-α smooth muscle actin (SMA) (1:400) alongside a goat anti-mouse polymer horseradish peroxidase (HRP) antibody followed by DAB detection (Envision+, Dako, K4007). Microarrays were also stained with rabbit antibodies against TNC (1:200), OPN (1:1000), EGF (1:500) and MMP-2 (1µg/ml) alongside goat anti-rabbit polymer alkaline phosphatase (AP) (1:500, Sigma, A3687) followed by Vulcan Fast Red detection (Cedarlane, FR805H). Microarrays were scanned using the Zeiss Mirax Midi slide scanner (Zeiss, Gottingen, Germany) and arteries were detected based on location, morphology and expression of SMA.

PAs were distinguished from pulmonary veins based on their location, structure, and expression profile of SMA (Zhao et al. 2005). PCNA and caspase-3 immunolabelings were quantified through positive cell counts from 10 arteries measuring under 45um in external diameter per lung with 7 lungs per group. These results were expressed as a percentage of positive cells compared to the total cell number. As for TNC, OPN, and EGF

immunolabelings, arteries were located using the bright field scans of each microarray and PAs were then isolated and cropped in the corresponding fluorescent image. Fluorescence intensity in the cropped images was computed using Zen software (Carl Zeiss Microscopy GmbH, Deutschland) and fitted into mean pixel intensity multiplied by pixel area divided by area of arterial wall. Ten arteries per lung sample, using 7 lung samples per group, were quantified. The average size of the PAs, for each immunolabeling quantified, was ensured to be not significantly different between the three groups (Ctl, CDH-, and CDH+).

2.7 Morphometric assessments

Morphometric assessments were performed using Mirax Viewer (Zeiss, Gottingen, Germany) on a tissue microarray labeled for SMA. Medial wall thickness, lumen area, vessel density, and vessel muscularization were quantified as outlined below.

2.8 Medial wall thickness quantification

PVD is associated with increased medial wall thickness of distal PAs – a structural characteristic that was calculated by averaging 5 measurements between the inner elastic lamina and outer boundary of the smooth muscle layer. Medial wall thickness measurements were done on PAs of 10-25 µm and 25-35 µm in external diameter and involved 10 and 15 arteries per lung respectively with 7 lungs per group.

2.9 Lumen area quantification

Lumen area was defined as the area within the internal elastic lamina and was expressed as a percentage of the total external area (Farkas et al. 2014). Ten PAs from 7 lungs per dose group with an external diameter of 10-35 µm were analyzed.

2.10 Vessel density quantification

The number of vessels was quantified in 45 high power fields (40X magnification) per left lung, in 7 animals per group. Only PAs with an external diameter of less than 35 µm were counted.

2.11 Vessel muscularization quantification

PAs under 35 µm in external diameter from the left lungs of each fetal rat, 7 per group, were measured and categorized as either muscularized (with a complete medial coat of muscle), partially muscularized (with only a crescent of muscle), or non muscularized (no visible muscle) (Luong et al. 2011).

2.12 In situ zymography

Fetal rat left lungs were flash frozen in liquid nitrogen, embedded in Shandon Cryomatrix (Thermo Scientific, 6769006), sectioned to an 8µm thickness and stored on glass slides at -80^{o}C. The sections were first incubated with fluorometric enzyme substrates specific for elastases (Invitrogen, E12056) or MMPs (AnaSpec, 71155) for 1 and 1.5 hours respectively at 37^{o}C, with or without inhibitors; sivelestat (selective neutrophil elastase inhibitor; 0.5 mM, Sigma, S7198), serpina1 (serine protease inhibitor; 1 mg/ml, Sigma, A6150), elafin (a serine elastase inhibitor; 1 mg/ml Sigma, E7280) and GM6001 (broad spectrum MMP inhibitor; 0.5 mg/ml, Millipore, CC1100). The sections were then labeled with a Cy3-conjugated anti-α smooth muscle actin antibody (1:500, Sigma, C6198) for 1 hour at 37^{o}C and counterstained with DAPI (SouthernBiotech, 0100-20). Enzyme activity, green fluorescence, was quantified using cropped images of 10 arteries per lung and 6 lungs per group from scanned slides and the aforementioned Zen software to measure fluorescence intensity. Negative controls were done with the previously stated protocol substituting the substrate with the provided reaction buffer.

2.13 Bacterial transformation, DNA isolation, and subloning of myc-DDK tagged elafin and serpina1 Proteins

Elafin (Origene, RC203136) and serpina1 (Origene, RC202082) cDNA plasmids as well as lentiviral plasmids (Origene, PS100070) were incubated separately with DH5α Escherichia Coli (Life Technologies, 18265-017) for 30 minutes on ice, heat shocked at 42^{o}C for 45 seconds, and returned to ice for 2 minutes for bacterial transformation. The bacteria were then mixed with LB broth and incubated for 45 minutes at 37 ^{o}C followed by plating on agar with antibiotic resistance; 50 µg/ml kanamycin (Life Technologies, 11815-024) for elafin and serpina1 plasmids, 34 µg/ml chloramphenicol (Sigma-Aldrich, C0378) for the empty lentiviral plasmid, and 17 µg/ml chloramphenicol for elafin or serpina1 modified lentiviral plasmids). Bacterial colonies containing the appropriate plasmids were then amplified and plasmid DNA was extracted using a Plasmid Midi Kit (QIAGEN, 12143).

In order to create stable protein expression in a variety of cell lines, elafin and serpina1 genes were subcloned into a lentiviral plasmid constitutively expressing GFP. All plasmids contained EcoRI and XhoI restriction sites flanking the gene of interest or multiple cloning site. Briefly, elafin and serpina1 amplicons were created using colony polymerase chain reaction (PCR) whereby plasmid DNA from 1 µl of transformed bacterial culture in LB broth (Fischer Scientific, BP1426-2) was denatured at 94^{o}C, annealed at 50^{o}C, and extended at 68^{o}C for 45 cycles with sequencing primers and a PCR master mix (Promega, m7502) followed by PCR purification using the PCR purification kit (QIAGEN, 28104). Amplicons were then digested using high fidelity restriction enzymes EcoRI (New England Biolabs, R3101) and XhoI (New England Biolabs, R0146S) along with the lentiviral plasmid. Plasmids and PCR products were purified separately. Digested lentiviral plasmids

were incubated with either elafin or serpina1 digested amplicons and T4 ligase (New England Biolabs, M0202S) at 16^{o}C for 2 hours. The resulting ligation mixture was used to transform bacteria as previously described.

To isolate bacterial colonies transformed with the ligation mixture containing the appropriate elafin or serpina1 subcloned lentiviral plasmid, 5 colonies per gene were grown individually in LB broth containing 34 µg/ml chloramphenicol overnight. From this culture, 1 µl was used for colony PCR with the provided sequencing primers as previously mentioned. The resulting PCR mix was then purified and run on a 1% agarose gel (Bio-Rad, 161-3100) with 0.1 µl/ml of Gel Red (VWR, 89139-138). DNA bands were visualized under ultra-violet light and the appropriate colonies were then chosen based on the presence and mass of the elafin and serpina1 DNA amplicons and further expanded for plasmid DNA isolation as previously outlined.

2.14 Lentivirus particle production, isolation, and transduction

After DNA isolation of elafin and serpina1 lentiviral plasmids, human embryonic kidney (HEK) 293T cells were transfected using a lenti-viral packaging kit (Origene, TR30022), which included MegaTran, modified lentiviral plasmid, and packaging plasmids as per manufacturers instructions. Twelve hours post-transfection, the media was changed to high-glucose DMEM (Fisher, SH3002201) with 10% fetal calf serum (Life Technologies, 12483-020) and 100 U/mL penicillin and 100 µg/mL streptomycin (P/S) antibiotic. After 72 hours the media was harvested and centrifuged at 3000rpm for 5 minutes to remove cellular debris and filtered through a 0.45 µm filter. One volume of a polyethylene glycol solution (PEG-It) (System Biosciences, LV810A-1) was added to 4 volumes of lentiviral media and incubated at 4^{o}C for 24 hours. The resulting mixture was then centrifuged at 1500G for 30

minutes to pellet the viral particles, which were then resuspended in PBS with 25mM HEPES buffer and stored at -80^{o}C.

For transduction, MSCs (Life Technologies, S1601-100) and fibroblasts (ATCC, CCL-192) were plated in either alpha-MEM (Life Technologies, 32571-036) with 10% MSC qualified FCS (Life Technologies, 12662-011) and P/S antibiotics or F12 (ATCC, 30-2004) with 20% FCS with P/S antibiotics respectively. Both conditions were supplemented with 10 µg/ml of polybrene (Millipore, TR-1003-G) and appropriate viral particles for 24 hours twice in a 6 well plate.

2.15 Magnetic activated cell sorting

One technique, that could be utilized to further confirm any results obtained by immunohistochemical staining of fetal rat lungs, is magnetic activated cell sorting of whole lung homogenates. Instead of doing Western blots of whole lung lysates, magnetic activated cell sorting (MACS) would allow extraction of SMCs for a more accurate representation of the pulmonary vasculature. Briefly, flash frozen lungs from CDH+, CDH- and control rat pups were minced and digested in a PUCK solution (8 g/L NaCl, 0.4 g/L KCl, 0.012 g/L $CaCl_2$, 0.154 g/L $MgSO_4$-$7H_2O$, 0.155 g/L Na_2HPO_4,, 0.15 g/L KH_2PO_4, and 1.1 g/L glucose in distilled water) containing 1 mg/ml collagenase A for 30 minutes at 37^{o}C. The resulting cell suspension was filtered through a 70 µm filter (Fisher, 08-771-2), washed with PBS and incubated with PECAM-1 (1:200) and Muc1 (1:200, Abcam, ab45167) antibodies conjugated to a secondary antibody linked to magnetic beads (New England Bioloabs, S1431S) for 30 minutes at 4^{o}C. A magnet was then used to pull all positive cells to the side of the reaction tube while the negative fraction containing SMCs was removed. All fractions were then lysed and analyzed via western blotting as previously described.

2.16 Assessing elastolytic activity

One volume of elastolytic reaction buffer (5x) was mixed with 1 volume of protein extract from cell lysates or conditioned media (2 µg/µl), 1 volume of elastin fluorometric substrate (100ug/ml) and 2 volumes of pancreatic elastase (0.1 U/ml) all provided in the elastase diagnostic kit (Invitrogen, E12056) in a 96 well cell culture plate. Fluorescence was assessed every 15 minutes using a luminescence microplate reader (BioTek, Synergy 2SL).

2.17 APGAR scoring

To develop a humane endpoint for future inhibitor trials using the nitrofen-induced CDH rat model, since death as an endpoint was deemed inhumane, an APGAR score was created. Pups were naturally birthed, were tagged, and their health was monitored. Skin colour, breathing, spontaneous motor activity, and reactivity to stimulus were all scored from 0 to 2 where 2 represented a healthy status (Nogueira-Silva et al. 2012).

2.18 Statistical analysis

All data collection was performed in a blinded fashion. Data from multiple experiments are expressed as mean ± standard error, and statistical significance was determined using one-way ANOVA followed by Tukey post-hoc analysis.

Results

3.1 Fetal rats with nitrofen-induced CDH present with low body weights and LH

Using the same nitrofen-induced CDH rat model as previously outlined in this report, many groups choose to report only the effects seen in the left lung of rats exposed to nitrofen that developed CDH and the olive oil control group. However, about 40-50% of the fetal rats exposed to nitrofen are born without CDH. In this report, data from the CDH+ and CDH- fetal rats was gathered so that we could better understand the effects that are due to nitrofen alone and compare them to those linked to the diaphragmatic defect. As shown in Figure 1A, nitrofen-exposed fetal rats had reduced body weights compared to controls. Body weights were even lower in the CDH+ animals. As LH is a hallmark of CDH, the left lung weight to body weight ratio was measured. The left lung to body weight ratio was diminished in pups from nitrofen-treated dams by a factor of 1.2X (Fig. 1B), which may reflect nitrofen's general inhibitory effect on cell proliferation (Tong et al. 2007). However, the left lung to body weight ratio was found to be 1.5X lower in the CDH+ group (Fig. 1B) suggesting the diaphragmatic defect had an additive effect.

3.2 Fetal rats with CDH present with features of PVD

Since the aim of this study is to determine whether the proteolytic-dependent progression of PVD, that was identified as being pivotal in the regulation of primary PH (Cowan et al. 2000), is also activated in PVD secondary to CDH, we first wanted to confirm that fetal rats who develop CDH after exposure to nitrofen showed features of PVD. Features of PVD include muscularization of peripheral arteries, medial wall hypertrophy of muscular arterioles, loss of small precapillary arteries, and neointima formation contributing to the

lumen obstruction (Rabinovitch 2008). First, muscular wall thickness (MWT), as defined as the distance between the EC layer and the arterial adventitial layer where cells stained positively for SMA, of PAs ranging from 10-25 μm (Fig. 2A) and 25-35 μm (Fig. 2B) were measured. These measurements showed a significant increase in MWT in rats with CDH when compared to both controls. The lumen area normalized to total arterial area was also quantified and was reduced in animals with CDH (Fig. 2C) suggesting possible vasoconstriction or PASMC encroachment into the lumen. The degree of muscularization of PAs was then assessed and, as shown in Fig. 2D, most PAs 10-35 μm in diameter from control and CDH- rats were non-muscular with only a small percentage (~12-14%) being fully muscularized. This portion however was significantly increased (~20%) in fetal rats with CDH. As an additional vascular abnormality associated with PVD, we also measured the number of PAs under 35 μm in diameter in the left lungs of the three animal groups. As shown in Figure 2E, the vessel density was significantly reduced in fetal rats with CDH when compared to controls. Since PVD can lead to right ventricular hypertrophy, we also measured the RV/LV+S ratio. Interestingly, this ratio was augmented in pups from dams treated with nitrofen when compared to controls (Fig. 2F), which may reflect cardiac malformations due to nitrofen (Losty et al. 1999). However, the increase was even more dramatic in fetal rats with CDH (Fig. 2F). Altogether, these data sets indicate that fetal rats with CDH present with many features of PVD similar to the human condition (O'Toole et al. 1996) and that this model is thus relevant to study mechanisms involved in PVD using the nitrofen-induced model of CDH.

3.3 Equivalent PCNA, caspase-3, EGF, OPN, TNC, SMA, and MMP2 levels from whole left lung lysates between all treatment groups

Because we were able to confirm various structural features of PVD in the nitrofen treated pups with CDH we wanted to determine whether the pathogenesis of PVD was consistent with the mechanism previously described in the progression of primary PH. Whole left lungs, the lungs most affected by the diaphragmatic defect, from rats exposed to nitrofen with and without CDH, along with the olive oil controls, were homogenized in lysis buffer and run on a Western blot. All proteins were normalized to tubulin, which was used as a loading control. SMA (Fig. 3A) and inactive caspase-3 levels (Fig. 3B) were equivalent amongst all 3 treatment groups. Interestingly, active-caspase-3 levels (Fig. 3C) were significantly different between CDH+ and nitrofen treated non-CDH groups. OPN (Fig. 3E) and TNC (Fig. 3F), found to be upregulated due to increased MMP2 activity in primary PH (Cowan, Jones, and Rabinovitch 1999), were not found to be affected in left lung lysates by nitrofen or CDH when compared to controls. It was hypothesized that, since MMP2 levels and activities in PAs from a primary PH model were found to be induced and led to increased PASMC proliferation when compared to non-hypertensive controls, lysates from CDH+ lungs would contain increased active MMP2 (66kDa) and PCNA and decreased pro-MMP2 (72kDa) levels compared to controls. When normalized to tubulin active-MMP2 (Fig. 3H), pro-MMP2 (Fig. 3I) and PCNA (Fig. 3J) remained unchanged with the exposure to nitrofen and induction of a CDH defect. Finally, growth factor levels, as determined by EGF quantification, although elevated in the CDH+ group were not significantly altered by the CDH defect or nitrofen (Fig. 3L).

3.4 Increased proliferation and decreased apoptosis of vascular cells was seen in PAs of fetal rats with CDH

Since we were able to show that the smooth muscle wall thickness of distal PAs is increased in rats with CDH, we wanted to determine whether increased MWT was due to deregulation of SMC proliferation and/or apoptosis specifically within the pulmonary vasculature. To verify this hypothesis, left lung tissue arrays were immunolabeled with PCNA and caspase-3, and the percentage of positive vascular cells were quantified. As shown in Fig. 4A, there was slight, but significant, increase in PCNA-positive cells in PAs of fetal rats with CDH (~50%) when compared to control animals (~42%). On the other end, a significant decrease of apoptotic cells was seen in the PAs of rats with CDH (Fig. 4B, ~2.7% vs ~6.6%). These results suggest that, in fetal rats with CDH, the increase in proliferation and decrease in apoptosis of vascular cells contribute to the wall thickening of PAs associated with PVD.

3.5 Elevated elastolytic and MMP activities in PAs of fetal rats with CDH

Cowan et al. (Cowan, Jones, and Rabinovitch 2000) have previously shown that increased elastase, MMP, ECM protein deposition, and SMC proliferation have been correlated with progressive medial wall thickening in primary PH. In order to assess whether a similar pathway also occurs in PVD associated with CDH, we started by measuring MMP activity using in situ zymography, as it allowed specific assessment of enzyme activity within PAs. In addition to MMP-9, the fluorescent substrate used in this assay could also be cleaved by MMP-1, 2, 3, 7, 8, 12, 13 and 14 thus allowed the measurement of a broad spectrum of MMP activities. In situ zymography revealed that MMP activity in PAs of fetal rats with CDH was significantly increased, ~67% (Fig. 5A), and was inhibited by the broad spectrum MMP inhibitor, GM6001 (Cowan, Jones, and Rabinovitch 2000) (Fig. 5B). The resulting fluorescence was deemed highly specific to MMP activity, as the fluorescent signal

was non-existent in the absence of the fluorometric substrate. Using a fluorometric substrate for elastase, we found that elastolytic activity was also induced by up to 50% in PAs from the CDH+ group when compared to control animals (Fig. 5C). This activity was inhibited by the serine elastase inhibitor sivelestat (Aikawa et al. 2011), the serine protease inhibitor serpina1 (Gao and Ray 2010), and another serine elastase inhibitor, elafin (Fig. 5D). Again, the fluorescent signal was undetectable in the absence of substrate. Altogether, these results indicate that serine elastase and MMP activity are elevated in PAs of fetal rats with CDH.

3.6 EGF and OPN levels are elevated in PAs of fetal rats with CDH

Since it has been reported that increased expression of TNC, EGF and PCNA accompanied the development and progression of PVD in rats (Jones, Cowan, and Rabinovitch 1997) and that antisense TNC prevented the progression of vascular disease (Cowan, Jones, and Rabinovitch 2000), we set out to determine whether EGF and TNC levels were elevated in PAs of fetal rats with CDH. We found that EGF levels were increased by ~2 fold in rats with CDH compared to the control group (Fig. 6A).

TNC expression has been reported in the pulmonary vasculature of adult rodents however has also been found to be notably absent in fetal and infant rats (Jones and Rabinovitch 1997). To confirm this finding, left lung tissue arrays were labeled for TNC in order to determine whether it is induced in PASMCs of animals with CDH. TNC could not be detected in PAs of neither controls nor CDH+ fetal rats however it was abundant amongst alveolar cells (data not shown). Reduction of TNC expression using antisense TNC RNA was reported to cause a concomitant increase in OPN levels in PAs (Cowan, Jones, and Rabinovitch 2000). This effect was selective because other ECM proteins, such as fibronectin, collagen, and elastin were not upregulated (Cowan, Jones, and Rabinovitch

2000). OPN levels were thus quantified in the lung tissue arrays and were found to be significantly higher in PAs of lungs from rats with CDH when compared to controls (Fig. 6B).

3.7 MACS sorting can be used to enrich SMCs from lung tissue

Using immunohistochemistry and in situ zymography, we were able to show that elevated PCNA, EGF and OPN levels, along with decreased caspase-3 levels, were associated with an induction in both elastase and MMP activities within the PAs of fetal rats with CDH. To further confirm these findings a MACS approach could be utilized to enable the enrichment of SMCs from lung homogenates of experimental animals that could to be later used for Western blot analysis. Unfortunately, SMCs do not exhibit any unique cell surface antigens necessary for cell sorting techniques (Weber et al. 2011). Removing the other cells composing the lung parenchyma, leaving an enriched SMC population, may however be possible. Using PECAM-1 and MUC1 antibodies conjugated to magnetic beads in order to remove ECs, epithelial cells, pneumocytes, and alveolar cells led to a 2 fold increase in SMA expression when comparing the negative cell fraction to a whole lung fraction (Fig. 7). Therefore, performing Western blot analysis, following MACS, to probe for PCNA, caspase-3, EGF and OPN levels followed by gel zymography to assess elastolytic and MMP activities may confirm our results obtained by immunohistochemistry.

3.8 Cell lysates and conditioned media from Myc-Tagged elafin and serpina1 transfected and lentiviral infected HEK293T cells inhibit elastolytic activity

Since we were able to show increased elastase and MMP enzyme activities within PAs of fetal rats with CDH, we wanted to pursue targeting these enzymes in order to reverse

PVD secondary to CDH. We thus devised an approach whereby we will administer, systemically, elastase and MMP inhibitors sivelestat and GM6001. Another approach that we will be exploring involves the use of stem cells, in particular EPCs or MSCs, modified to expressed serine elastase inhibitor elafin or serine protease inhibitor serpina1. An animal protocol has already been established for future sivelestat and GM6001 therapies however preliminary work needed to be done in order to continue with the stem cell approach.

In order to move to animal trials using expressible inhibitors, elafin and serpina1, in stem cells, elafin and serpina1 needed to be tested and their genes stably inserted into the genomes of EPCs and MSCs. To begin, we decided to use myc-DDK tagged versions of elafin and serpina1 in order to be able to distinguish these proteins from their endogenous counterparts. We thus needed to confirm proper activity and secretion of the tagged proteins. To verify the activity and secretory properties of myc-DDK tagged elafin and serpina1, HEK293T cells were transiently transfected with cDNA plasmids containing the myc-DDK tagged elafin and serpina1 genes. Expression of elafin and serpina1, along with their myc-DDK tags, was verified using Western blot. It became apparent that tagged active elafin, although apparent in cell lysates, is heavily secreted into the media in both its inactive larger pre-elafin (trappin-2) and smaller active forms whereas tagged serpina1, although present in the media is more abundant in cell lysates and can be visualized as a doublet representing its phosphorylated and unphosphorylated states (Fig. 8A). Further characterization of the tagged elafin and serpina1 proteins showed that both transfected HEK293T lysates (Fig. 8B) and conditioned media (Fig. 8C) inhibited pancreatic elastase activity when compared to HEK293T lysates and media transfected with an empty GFP plasmid.

Tagged elafin and serpina1 genes within the cDNA plasmids were then subcloned into a lentiviral plasmid constitutively expressing GFP in order to create stable EPC and

MSC lines expressing the two inhibitors. Elafin and serpina1 secretion was once again confirmed in HEK293T cells transduced with lentiviral particles containing the lentiviral plasmids with the elafin and serpina1 genes (Fig. 9A). Elastase inhibition was again assessed against pancreatic elastase where cell lysates (Fig. 9B) and conditioned media, (Fig. 9C) from HEK293T cells transduced with elafin and serpina1, were found to be able to inhibit elastase activity compared to an empty plasmid control. Inhibition of pancreatic elastase by cell lysates and media from cells infected with elafin and serpina1 was significant yet low. Although it is not expected that HEK293T cells express serine protease inhibitors it is known that they express two serine proteases OMI (GenBank: AF184911.1) and PRSS25 (GenBank: AF141305.1). Using an elafin and serpina1 infected cell line that is known not to express serine proteases, such as baby hamster kidney (BHK) (Kratje, Lind, and Wagner 1994) may show greater pancreatic elastase inhibition. Also, culturing cells in serum free media would negate serum mediated elastase inhibition since serum is known to contain trace amounts of serpina1 (Shapiro, Pott, and Ralston 2001).

3.9 An APGAR score of 1 can predict imminent death in rat pups within 10-20 minutes

As previously mentioned, one approach to inhibiting the induced matrix enzyme activity in PAs of fetal rats with CDH and to reverse PVD was with the use of sivelestat and GM6001. One of the ways we planned to assess the effectiveness of this treatment was by survival times. After submitting an animal protocol for testing the use of sivelestat and GM6001 with our nitrofen induced CDH rat model the Animal Care Committee at the University of Ottawa suggested that using death as an endpoint is unethical and therefore unacceptable. We therefore suggested using an APGAR score that could consistently predict

imminent death in rat pups as a more ethical approach. It was found that an APGAR score of 1 could be accurately measured and was able to predict imminent death within 10-20 minutes (Fig. 10). Interestingly, it was also found that pups exposed to nitrofen with CDH died within 1 hour after birth and pups exposed to nitrofen that did not exhibit a diaphragmatic defect all died within 15 hours after birth (Fig. 10).

Discussion

4.1 A need for a treatment targeting PVD associated with CDH

To date, treatments for PH secondary to CDH have shown limited success and CDH continues to be one of the greatest difficulties for perinatal medicine (Gerben, Alan, and Bruce 2003). Currently, the standard practice in many children's hospitals involves stabilization of infants immediately upon birth with ventilators infused with nitric oxide (NO) to stimulate vasodilation and reduce blood pressure followed by diaphragmatic patch surgery (Bagolan et al. 2004). Unfortunately, the high mortality and morbidity rates associated with CDH remain (Group 1997). It is hypothesized that treating the PH secondary to CDH is necessary for the improved stabilization of infants with CDH and may lead to increases in the number of patients who survive until surgery and lower the morbidity associated with the condition. Interestingly, serine elastase inhibition has been shown to induce complete reversal of fatal primary PH in rats, increase survival through arrest of TNC accumulation and proliferation, and induce apoptosis and resorption of the abundant ECM (Cowan et al. 2000). The rationale came from the demonstration that increased elastase and MMP activity and deposition of TNC, codistributing with proliferating SMCs, are features of PH (Ihida-stansbury et al. 2006; Jones, Cowan, and Rabinovitch 1997) and that regression of hypertrophied rat PAs in organ culture is associated with suppression of proteolytic activity, inhibition of TNC, and SMC apoptosis (Cowan, Jones, and Rabinovitch 2000). Therefore, treating patients with serine elastase and MMP inhibitors may also lead to disease reversal, decreased time to full stabilization, and increased survival.

4.2 Confirming induced matrix enzyme activity and downstream molecular pathway in the nitrofen induced CDH rat model

One of the aims of this study was to verify whether the progression of PVD associated with CDH shares a similar pathogenesis as primary PH as detailed by Cowan et al, 2000. First, we started with the nitrofen induced CDH rat model because it is a well established experimental model that mimics the major abnormalities and pathology described in the human CDH condition (Luong et al. 2011; Susan et al. 1983). Using whole left lung lysates of nitrofen fed CDH and non-CDH pups along with olive oil fed controls we probed for PCNA, caspase-3, EGF, OPN, TNC, MMP2, and SMA. We expected increased PCNA, EGF, TNC and MMP2 levels in lysates from CDH affected pups. Unfortunately there were no observable changes in any protein or growth factor levels between the 3 groups. It was then thought that the total protein and growth factor levels within the entire lung parenchyma might mask any changes specific to the pulmonary vasculature. To address this issue we embedded 21 left lungs, 7 per treatment group, in a tissue microarray and utilized immunohistochemistry to identify all of the aforementioned proteins and EGF. Using a tissue microarray, all lung sections were on one slide and therefore treated equivalently allowing direct comparison between CDH+, CDH- and control lungs. We found that increased PCNA and decreased caspase-3 concomitant with increased EGF and OPN was observable specifically within the pulmonary vascular system. Further analysis using in situ zymography found that elastase and MMP activity was also induced in PAs of rats with CDH.

To provide further evidence supporting our immunohistochemistry and in situ zymography results a multitude of methods could be used, all of which present with unique challenges. Using MACS to isolate and enrich a lung fraction for SMCs would enable us to potentially unmask the changes in protein and growth factor levels, seen in the pulmonary vasculature using immunohistochemistry, by removing unwanted cell types from lung lysates. Gel zymography could then also be used to assess elastase and MMP activity. The

challenge with this approach is SMCs do not present a unique cell surface antigen as needed for cell separation. Removing most other cell types would be possible however obtaining a pure source of SMCs from lung tissue is currently not feasible (Weber et al. 2011). Also, isolation of PASMCs from SMCs lining the respiratory tract would not be possible. Another conceivable approach would be using laser microdissection to isolate PAs followed by quantitative PCR analysis for PCNA, caspase-3, EGF, OPN, TNC, and MMP2. Limitations to this technique include the inability to quantify protein levels or assess enzyme activity. Correlation between RNA transcript levels and protein expression and activity can be as low as 40% depending on the research model and protein of interest (Vogel and Marcotte 2012) and therefore may not provide reliable data to confirm our immunohistochemical results. Although immunohistochemistry has provided us with concrete evidence to support our hypothesis recapitulating our results is necessary. Doing so with the use of PA organ explants or MACS to enrich SMCs within the lung seem to be the best two options available at this point in time.

4.3 Assessing effects and mechanism of serine elastase inhibition may lead to a greater understanding of PH pathogenesis

The study of PASMCs associated with PVD has been undertaken by many groups worldwide and has yielded a plethora of mechanisms and potential therapeutic approaches all with varying degrees of success. To date little has been done to link pathogenesis models of PH together although it is expected that many are in fact interconnected as many phenotypes consistent among all PH models have been observed. It has been identified that PASMCs grown under hypoxic conditions exhibit a depolarized phenotype compared to cells grown under normoxic conditions (Shimoda and Polak 2011; J. Yuan et al. 1998). One reason for

persistent partial depolarization stems from decreased K^+ channel expression and activity. It was found that dehydroepiandrosterone, a steroid hormone known to open K^+ channels, successfully reduced the amount of vascular remodeling in rats living under hypoxic conditions or treated with monocrotaline (Bonnet et al. 2003; McMurtry et al. 2004).

Other phenotypes observed in PH-associated PASMCs include a faulty sodium-hydrogen antiporter (NHE), specifically NHE1, and increased internal calcium ion concentrations ($[Ca^{+2}]_i$). NHE1 is a membrane transport protein involved in pH homeostasis and cell volume regulation in vertebrate cells. Unfortunately NHE1 inhibitors show major side effects including cerebrovascular events as NHE1 is expressed in all cell types (Mentzer et al. 2008). Since pH (NHE1 activity) and degree of cell polarization (K^+ channel activity) are known to affect $[Ca^{+2}]_I$, and due to the dependence of PASMCs on Ca^{+2} signaling to initiate proliferation and migration, $[Ca^{+2}]_i$ was assessed and confirmed to be elevated in PASMCs affected by hypoxic conditions (Leggett et al. 2012). Sildenafil successfully reduced $[Ca^{+2}]_i$, led to attenuation of hypoxia induced PASMC proliferation, and prevented remodeling in the monocrotaline animal model (Wharton et al. 2005; J. Yang et al. 2013).

Interestingly, activation of RhoA+B, essential to the ROCK pathway, has been shown to increase NHE1 and open $[Ca^{+2}]_i$ channels thereby supporting the premise that pH homeostasis and $[Ca^{+2}]_i$ play a substantial role in the progression of PH (Luke et al. 2012). Also, BMP2+4 are antiproliferative in proximal PASMCs but increase $[Ca^{+2}]_i$ and proliferation in distal PASMCs (X. Yang et al. 2005). Finally, a vasoconstrictor, ET-1, binds to ET_A and ET_B membrane receptors and results in inhibition of K^+ channels, increased $[Ca^{+2}]_i$, and activation of NHE1 (Shimoda et al. 2002; Undem et al. 2012; Whitman et al. 2008). Inhibition of K^+ channels, increased $[Ca^{+2}]_i$, and activation of NHE1 thus seem to be effects of a multitude of PH causing mechanisms. It could therefore be hypothesized that

inhibition of serine elastase activity, as we have shown to be induced in the pulmonary vasculatures of fetal rats with CDH, may cause increases in K^+ channel activity, decreases in $[Ca^{+2}]_i$, and deactivation of NHE1. This may aid in determining the pathogenesis of PVD.

It is likely that many of the aforementioned mechanisms responsible for the progression of PH function coherently or even synergistically with each other. For example it is known that ET-1, a potent vasoconstrictor, also is able to activate ROCK signaling (Whitman et al. 2008). Another phenotype associated with PH is decreased NO, a vasodilator, caused by decreases in eNOS activity in ECs (Zhao et al. 2005). Increasing NO levels within the pulmonary vasculature by administering EPCs expressing eNOS lead to a complete reversal of monocrotaline induced PH in rats (Zhao et al. 2005). Interestingly, it has been shown that increases in NO levels reduces PASMC elastase activity (Mitani et al. 2000). Therefore, exploring the effects of serine elastase inhibition on induced elastase activity seen in PAs of fetal rats with CDH alongside the effects on the pathways previously identified to be associated with PH may provide greater understanding of the interconnectivity and overall mechanism associated with the pathogenesis of PH.

4.4 Treating PVD with sivelestat and GM6001

Our study has found that increased vascular cell proliferation and decreased apoptosis concomitant with increased EGF and OPN levels and increased serine elastase and MMP activity was associated with the PVD triggered by CDH. One of the aims of this study was to assess whether inhibition of the induced matrix enzyme pathway would result in reversal of PVD and increased survival in CDH affected patients. One of the approaches this lab will be studying in the future is the use of sivelestat, a serine elastase inhibitor and GM6001, an MMP inhibitor, on PVD associated with CDH. When determining an appropriate APGAR

score for an ethical end point in the sivelestat GM6001 study it was found that all CDH+ pups died within an hour after birth and all CDH- pups died within 15 hours after birth. Since the onset of action of small molecules usually ranges between 20 and 60 minutes and since it takes much longer to produce an observable phenotypic effect it became apparent that pups with CDH will have to be treated both pre and postnatally (Pang 2003). Maternal rats will have to be exposed to sivelestat and GM6001 followed by the pups once born. Unfortunately, it is unknown whether sivelestat and GM6001 are capable of crossing the placenta. Performing whole lung elastase inhibitory assays, first on treated and untreated mother rat lungs to establish a positive control and then on the treated and untreated pups will allow proper determination of whether sivelestat and GM6001 cross the placenta and affect lung elastase levels. An ELISA detecting fetal blood serine elastase inhibition could also be performed to assess whether the two small molecules can cross the placenta. Once confirmed animal trials may begin.

If proven successful it would not be the first time these compounds were used in a human setting. Trials for the use of sivelestat and GM6001 against systemic inflammatory response syndrome due to acute lung injury and corneal ulcerations respectively in humans have been previously undertaken with sivelestat being approved for public consumption and GM6001 in phase II clinical trials (Galardy et al. 1994; Iwata et al. 2010). Research is currently being done on the long-term side effects of sivelestat however current trials on have not found significant difficulties in patients treated with these drugs (Aikawa et al. 2011). GM6001, on the other hand, may exhibit detrimental long-term side effects as is the case with other MMP inhibitors, which have been tested rigorously as anti-cancer therapeutics (Coussens, Fingleton, and Matrisian 2002). Therefore, the use of sivelestat and GM6001 in human patients with CDH may be a possibility in the future.

4.5 Using MSCs and EPCs expressing elafin and serpina1 to target and reverse PVD

Unfortunately, the side effects of systemically administering sivelestat and GM6001 to infants have not yet been elucidated and it currently remains unknown whether the two drugs can cross the placenta, a necessity for prenatal drug administration for our nitrofen-induced CDH rat model. We therefore began exploring a more targeted approach for the delivery of protease inhibitors through the use of stem cells, in particular EPCs and MSCs, genetically enhanced to produce elafin and serpina1. A study using EPCs modified to express eNOS has already shown a complete reversal of monocrotaline induced primary PH (Zhao et al. 2005) and therefore provides, along with the results obtained in this study, the proof of principle for our approach towards treating PVD associated with CDH.

Elafin and serpina1, also known as α-1 antitrypsin, are naturally secreted serine elastase and serine protease inhibitors respectively (Shaw and Wiedow 2011; Wewers and Crystal 2013). Elafin and serpina1 augmentation therapies, currently in phase II and III clinical trials have been well tolerated with little to no signs of significant side effects (Shaw and Wiedow 2011; Wewers and Crystal 2013). Since these two inhibitors are naturally secreted we needed a way to distinguish natural from artificially added elafin and serpina1 to assess treatment efficacy. We therefore set out to create elafin and serpina1 proteins conjugated to a myc-DDK tag. Although untagged elafin and serpina1 proteins have already been confirmed to inhibit the induced elastolytic activity seen in PAs of fetal rats with CDH we needed and were able to confirm that elafin and serpina1 conjugated to a myc-DDK tag maintained their secretory properties and inhibitory activities. Lentiviral particles containing tagged elafin and serpina1 plasmid DNA which also expressesd GFP were created and could

be used to infect EPCs and/or MSCs to create stable cell lines for future ultrasound guided intrautero intracardiac, intrauterine, or intraperitoneal injection into fetal rats with nitrofen induced CDH. Although rat derived MSCs are notoriously difficult to transduce, human MSCs are much more receptive to lentiviral plasmid DNA incorporation (Lin et al. 2012; Ricks et al. 2008). Therefore FACS targeting GFP expressing cells could be used to isolate pure rat stem cell colonies expressing elafin or serpina1.

To ensure proper homing of EPCs and MSCs to the lungs of fetal rats with CDH we will be utilizing EPCs and MSCs modified with lentiviral plasmids that constitutively express GFP. Once cells are injected into the fetal rats it may be possible to locate their GFP signals using IVIS200 imaging. We could also sacrifice pups at different time stages, collect and section their organs, and perform immunohistochemistry using an anti-GFP antibody to confirm therapeutic stem cell presence. These methods will also be able to help us compare and optimize the stem cell injection method best suited for a treatment for PVD.

4.6 Concluding remarks

Collectively, the results from this study suggest that the progression of PVD associated with CDH involves an increase in proliferation and a decrease in apoptosis in PAs of fetal rats with CDH that is accompanied by an induction of elastase and MMP activity and OPN levels, in an EGF-rich environment. As inhibition of elastase and MMP activity (Cowan et al. 2000), as well as EGF receptor blockade (S. L. Merklinger et al. 2005), have been shown to improve survival in rats with primary PH, the molecular players identified here may thus represent potential new therapeutic targets for the treatment of PVD associated with CDH. This ongoing project is part of our translational research program with the

ultimate goal of developing a novel strategy of targeting PH in infants with CDH to improve survival and long-term outcome.

References

Aikawa, N. et al. 2011. "Reevaluation of the Efficacy and Safety of the Neutrophil Elastase Inhibitor, Sivelestat, for the Treatment of Acute Lung Injury Associated with Systemic Inflammatory Response Syndrome; a Phase IV Study." *Pulmonary pharmacology & therapeutics* 24(5): 549–54.

Allan, JA. et al. 1995. "Binding of Gelatinases A and B to Type-I Collagen and Other Matrix Components." *Biochem J* 309: 299–306.

Anderson, DH. 1941. "Incidence of Congenital Diaphragmatic Hernia in the Young of Rats Bred on a Diet Deficient in Vitamin." *Am J Dis Child* 62: 888–89.

Anderson, DH. 1949. "Effect of Diet during Pregnancy upon the Incidence of Congenital Hereditary Diaphragmatic Hernia in the Rat." *Am J Path* 25: 163–85.

Aubry, E. et al. 2013. "Tracheal Occlusion Alters Pulmonary Circulation in the Fetal Lamb with Normally Developing Lungs." *J Pediatr Surg* 48(3): 481–87.

Babiuk, RP. et al. 2002. "Embryological Origins and Development of the Rat Diaphragm." *Journal of Comparative Neurology* 455(4): 477–87.

Bagolan, P. et al. 2004. "Impact of a Current Treatment Protocol on Outcome of High-Risk Congenital Diaphragmatic Hernia." *Journal of Pediatric Surgery* 39(3): 313–18.

Bartsch, S. et al. 1992. "Expression of Tenascin in the Developing and Adult Cerebellar Cortex." *J Neurosci* 12: 736–49.

Berg, JT. 2007. "Chronic Hypoxia-Induced Pulmonary Hypertension Does/does Not Lead to Loss of Pulmonary Vasculature." *J Appl Physiol* 103: 1455.

Bladt, F. et al. 1995. "Essential Role for the c-Met Receptor in the Migration of Myogenic Precursor Cells into the Limb." *Nature* 376: 768–71.

Bohn, D. 2002. "Congenital Diaphragmatic Hernia." *J Respir Crit Care Med* 166: 911–15.

Bonnet, S. et al. 2003. "Dehydroepian-Drosterone (DHEA) Prevents and Reverses Chronic Hypoxic Pulmonary Hypertension." *Proc Natl Acad Sci U S A* 100: 9488–93.

Botney, MD. et al. 1992. "Extracellular Matrix Protein Gene Expression Inatherosclerotic Hypertensive Pulmonary Arteries." *Am J Pathol* 140: 357–64.

Brown, TJ., and JM. Manson. 1988. "Further Characterization of the Distribution and Metabolism of Nitrofen in the Pregnant Rat." *Teratology* 34(2): 129–39.

Brownlee, EM., AG. Howatson, CF. Davis, and AJ. Sabharwal. 2009. "The Hidden Mortality of Congenital Diaphragmatic Hernia: A 20-Year Review." *J Pediatr Surg* 44(2): 317–20.

Bussolati, B. 2011. "Stem Cells for Organ Repair." *Organogenesis* 7(2): 95.

Chang, YS. et al. 2009. "Human Umbilical Cord Blood-Derived Mesenchymal Stem Cells Attenuate Hyperoxia-Induced Lung Injury in Neonatal Rats." *Cell Transplant* 18(8): 869–86.

Chaput, N., and C. Théry. 2011. "Exosomes: Immune Properties and Potential Clinical Implementations." *Semin Immunopathol* 33: 419–40.

Chiu, PP. et al. 2006. "The Price of Success in the Management of Congenital Diaphragmatic Hernia: Is Improved Survival Accompanied by an Increase in Long-Term Morbidity?" *J Pediatr Surg* 41(5): 888–92.

Clugston, RD. et al. 2006. "Teratogen-Induced, Dietary and Genetic Models of Congenital Diaphragmatic Hernia Share a Common Mechanism of Pathogenesis." *Am J Pathol* 169(5): 1541–49.

Cohen, JC., and JE. Larson. 2008. "The Peter Pan Paradigm." *Theoretical Biology and Medical Modelling* 5(1): 1–6.

Costlow, RD., and JM. Manson. 1981. "The Heart and Diaphragm: Target Organs in the Neonatal Death Induced by Nitrofen (2,4-Dichlorophenyl-P-Nitrophenyl Ether)." *Toxicology* 20: 209–27.

Coussens, LM., B. Fingleton, and LM. Matrisian. 2002. "Matrix Metalloproteinase Inhibitors and Cancer: Trials and Tribulations." *Science* 295(5564): 2387–92.

Cowan, KN. et al. 2000. "Complete Reversal of Fatal Pulmonary Hypertension in Rats by a Serine Elastase Inhibitor." *Nature medicine* 6(6): 698–702.

Cowan, KN., PL. Jones, and M. Rabinovitch. 1999. "Regression of Hypertrophied Rat Pulmonary Arteries in Organ Culture Is Associated With Suppression of Proteolytic Activity, Inhibition of Tenascin-C, and Smooth Muscle Cell Apoptosis." *Circulation Research* 84(10): 1223–33.

Cowan, KN., PL. Jones, and M. Rabinovitch. 2000. "Elastase and Matrix Metalloproteinase Inhibitors Induce Regression, and Tenascin-C Antisense Prevents Progression, of Vascular Disease." *J. Clin. Invest.* 105: 21–34.

Davie, NJ. et al. 2009. "The Science of Endothelin-1 and Endothelin Receptor Antagonists in the Management of Pulmonary Arterial Hypertension: Current Understanding and Future Studies." *Eur J Clin Investig* 38S2: 38–49.

Davies, RJ., and NW. Morrell. 2008. "Molecular Mechanisms of Pulmonary Arterial Hypertension: Role of Mutations in the Bone Morphogenetic Protein Type II Receptor." *Chest* 134: 1271–77.

Dekoninck, P. et al. 2011. "Results of Fetal Endoscopic Tracheal Occlusion for Congenital Diaphragmatic Hernia and the Set up of the Randomized Controlled TOTAL Trial." *Early Hum Dev.* 87(9): 619–24.

Downard, CD. et al. 2003. "Analysis of an Improved Survival Rate for Congenital Diaphragmatic Hernia." *J Pediatr Surg* 38(5): 729–32.

Enns, GM. et al. 1998. "Congenital Diaphragmatic Defects and Associated Syndromes, Malformations, and Chromosome Anomalies: A Retrospective Study of 60 Patients and Literature Review." *Am J Med Genet* 79: 215–25.

Farkas, D. et al. 2014. "CXCR4 Inhibition Ameliorates Severe Obliterative Pulmonary Hypertension and Accumulation of C-Kit+ Cells in Rats." *PloS ONE* 9: e89810.

Fung, ME., and B. Thébaud. 2014. "Stem Cell–based Therapy for Neonatal Lung Disease: It Is in the Juice." *Pediatric Research* 75(1): 2–7.

Galardy, RE. et al. 1994. "Low Molecular Weight Inhibitors in Corneal Ulceration." *Annals of the New York Academy of Sciences* 732: 315–23.

Gan, CTJ. et al. 2007. "Noninvasively Assessed Pulmonary Artery Stiffness Pre- Dicts Mortality in Pulmonary Arterial Hypertension." *Chest* 132(6): 1906–12.

Gangopahyay, A. et al. 2011. "Bone Morphogenetic Protein Receptor II Is a Novel Mediator of Endothelial Nitric-Oxide Synthase Activation." *J Biol Chem* 286: 33134–40.

Gao, Y., and JU. Ray. 2010. "Regulation of the Pulmonary Circulation in the Fetus and Newborn." *Circulation* 90(480): 1291–1335.

Gerben, S., F. Alan, and J. Bruce. 2003. "Nihilism in the 1990s: The True Mortality of Congenital Diaphragmatic Hernia." *Pediatrics* 112(3): 532–35.

Gosemann, JH. et al. 2013. "Disruption of the Bone Morphogenetic Protein Receptor 2 Pathway in Nitrofen-Induced Congenital Diaphragmatic Hernia." *Birth Defects Research Part B* 98(4): 304–9.

Greer, JJ. 2013. "Current Concepts on the Pathogenesis and Etiology of Congenital Diaphragmatic Hernia." *Respir Physiol Neurobiol* 189: 232–40.

Greer, JJ., DW. Allan, RP. Babiuk, and R. Clugston. 2005. "Insights into the Pathogenesis and Etiology of Congenital Diaphragmatic Hernia from Rodent Models." *Fetal and Maternal Medicine Reviews* 16(3): 211–20.

Greer, JJ., RP. Babiuk, and B. Thebaud. 2003. “Etiology of Congenital Diaphragmatic Hernia: The Retinoid Hypothesis.” *Pediatric Research* 53: 726–30.

Griffiths, MJ., D. Bonnet, and SM. Janes. 2005. “Stem Cells of the Alveolar Epithelium.” *Lancet* 366: 249–60.

Group, The Neonatal Inhaled Nitric Oxide Study. 1997. “Inhaled Nitric Oxide and Hypoxic Respiratory Failure in Infants with Congenital Diaphragmatic Hernia.” *Pediatrics* 99(6): 838–45.

Guilluy, C. et al. 2005. “Inhibition of RhoA/Rho Kinase Pathway Is Involved in the Beneficial Effect of Sildenafil on Pulmonary Hypertension.” *Br J Pharmacol* 146: 1010–18.

Hansmann, G. et al. 2012. “Mesenchymal Stem Cell-Mediated Reversal of Bronchopulmonary Dysplasia and Associated Pulmonary Hypertension.” *Pulm Circ* 2(2): 170–81.

Hopper, AF., and NH. Hart. 1985. *Foundations of Animal Development.* Oxford: Oxford University Press.

Horwitz, M. et al. 1999. “Mutations in ELA2, Encoding Neutrophil Elastase, Define a 21-Day Biological Clock in Cyclic Haematopoiesis.” *Nat. Genet* 23(4): 433–36.

Hur, J. et al. 2007. “Akt Is a Key Modulator of Endothelial Progenitor Cell Trafficking in Ischemic Muscle.” *Stem Cells* 25: 1769–78.

Ihida-stansbury, Kaori et al. 2006. “Tenascin-C Is Induced by Mutated BMP Type II Receptors in Familial Forms of Pulmonary Arterial Hypertension.” 6383: 694–702.

Ionescu, L. et al. 2012. “Stem Cell Conditioned Medium Improves Acute Lung Injury in Mice: In Vivo Evidence for Stem Cell Paracrine Action.” *Am J Physiol Lung Cell Mol Physiol* 303(11): L967–77.

Iwata, K. et al. 2010. “Effect of Neutrophil Elastase Inhibitor (sivelestat Sodium) in the Treatment of Acute Lung Injury (ALI) and Acute Respiratory Distress Syndrome (ARDS): A Systematic Review and Meta-Analysis.” *Internal medicine* 49(22):

Jones, PL. et al. 1995. “TenascinC Inhibits Extra Cellular Matrix-Dependent Gene Expression in Mammary Epithelial Cells: Localization of Active Regions Using Recombinant Tenasc in Fragments.” *J Cell Sci* 108: 519–27.

Jones, PL., KN. Cowan, and M. Rabinovitch. 1997. “Tenascin-C, Proliferation and Subendothelial Fibronectin in Progressive Pulmonary Vascular Disease.” *The American journal of pathology* 150(4): 1349–60.

Jones, PL., J. Crack, and M. Rabinovitch. 1997. “Regulation of Tenascin-C, a Vascular Smooth Muscle Cell Survival Factor That Interacts with the avb3 Integrin to Promote Epidermal Growth Factor Receptor Phosphorylation and Growth.” *The Journal of Cell Biology* 139: 279–93.

Jones, PL., and M. Rabinovitch. 1997. “Tenascin-C Is Induced with Progressive Pulmonary Vascular Disease and Is Functionaly Related to Increased Smooth Muscle Cell Proliferation.” *Circ Res* 79: 1131–42.

Kawamoto, A.. et al. 2004. “Synergistic Effect of Bone Marrow Mobilization and Vascular Endothelial Growth Factor-2 Gene Therapy in Myocardial Ischemia.” *Circulation* 110(11): 1398–1405.

Kays, DW. 2006. “Congenital Diaphragmatic Hernia and Neonatal Lung Lesions.” *Surg Clin North Am* 86(2): 329–52.

Keijzer, R. 2010. “Congenital Diaphragmatic Hernia.” *Seminars in Pediatric Surgery* 19: 180–85.

Kim, CF. et al. 2005. “Identification of Bronchioalveolar Stem Cells in Normal Lung and Lung Cancer.” *Cell* 121(6): 823–35.

Kinsella, JP., DD. Ivy, and SH. Abman. 2005. “Pulmonary Vasodilator Therapy in Congenital Diaphragmatic Hernia: Acute, Late, and Chronic Pulmonary Hypertension.” *Semin Perinatol* 29: 123–28.

Kluth, D. et al. 1993. “The Natural History of Congenital Diaphragmatic Hernia and Pulmonary Hypoplasia in the Embryo.” *Journal of Pediatric Surgery* 28(3): 456–62.

Kotecha, S. et al. 2012. “Congenital Diaphragmatic Hernia.” *European Respiratory Jour nal* 39(4): 820–29.

Kratje, RB., W. Lind, and R. Wagner. 1994. “Evaluation of the Proteolytic Potential of in Vitro-Cultivated Hybridoma and Recombinant Mammalian Cells.” *Journal of biotechnology* 32(2): 107–25.

Kutasy, B. et al. 2014. “Nitrofen Increases Total Retinol Levels in Placenta during Lung Morphogenesis in the Nitrofen Model of Congenital Diaphragmatic Hernia.” *Pediatr Surg Int*: [Epub ahead of print].

Lamouille, S., J. Xu, and R. Derynck. 2014. “Molecular Mechanisms of Epithelial–mesenchymal Transition.” *Nature Reviews Molecular Cell Biology* 15: 178–96.

Langham, MR. et al. 1996. “Congenital Diaphragmatic Hernia. Epidemiology and Outcome.” *Clin Perinatol* 23(4): 671–88.

Lee, C. et al. 2012. “Exosomes Mediate the Cytoprotective Action of Mesenchymal Stromal Cells on Hypoxia-Induced Pulmonary Hypertension.” *Circulation* 126(22): 2601–11.

Leggett, K. et al. 2012. “Hypoxia-Induced Migration in Pulmonary Arterial Smooth Muscle Cells Requires Calcium-Dependent Upregulation of Aquaporin 1.” *Am J Physiol Lung Cell Mol Physiol* 303: L343–53.

Lin, P. et al. 2012. “Efficient Lentiviral Transduction of Human Mesenchymal Stem Cells That Preserves Proliferation and Differentiation Capabilities.” *Stem cells translational medicine* 1(12): 886–97.

Logan, JW., HE. Rice, RN. Goldberg, and CM. Cotten. 2007. “Congenital Diaphragmatic Hernia: A Systematic Review and Summary of Best-Evidence Practice Strategies.” *J Perinatol* 27(9): 535–49.

Losty, PD. et al. 1999. “Malformations in Experimental Diaphragmatic Hernia.” *Journal of Pediatric Surgery* 34(8): 1203–7.

Lowery, JW., and MP. de Caestecker. 2010. “BMP Signaling in Vascular Development and Disease.” *Cytokine Growth Factor Rev* 21: 287–98.

Luke, T. et al. 2012. “Kinase Dependent Activation of Voltage-Gated Ca2+ Channels by ET-1 in Pulmonary Arterial Myocytes during Chronic Hypoxia.” *Am J Physiol Lung Cell Mol Physiol* 302: L1128–39.

Lunn, R. 2011. *Report on Carcinogens; 12th Ed. U. S. Department of Health and Human Services.*

Luong, C. et al. 2011. “Antenatal Sildenafil Treatment Attenuates Pulmonary Hypertension in Experimental Congenital Diaphragmatic Hernia.” *Circulation* 123(19): 2120–31.

Mahapatra, S. et al. 2006. “Relationship of Pulmonary Arterial Capacitance and Mortality in Idiopathic Pulmonary Arterial Hypertension.” *J Am Coll Cardiol* 47: 799–803.

Major, D. et al. 1998. “Retinol Status of Newborn Infants with Congenital Diaphragmatic Hernia.” *Pediatr Surg Int* 13: 547–49.

Malpel, S., C. Mendelsohn, and WV. Cardoso. 2000. “Regulation of Retinoic Acid Signaling during Lung Morphogenesis.” *Development* 127: 3057–67.

Manson, JM. 1986. “Mechanism of Nitrofen Teratogenesis.” *Environ Health Perspect.* 70: 137–47.

Martin, E. et al. 2012. “Involvement of TRPV1 and TRPV4 Channels in Migration of Rat Pulmonary Arterial Smooth Muscle Cells.” *Pflugers Arch* 464: 261–72.

McMurtry, MS. et al. 2004. “Dichloroacetate Prevents and Reverses Pulmonary Hypertension by Inducing Pulmonary Artery Smooth Muscle Cell Apoptosis.” *Circ Res* 95: 830–40.

Mentzer, RM. et al. 2008. “Sodium-Hydrogen Exchange Inhibition by Cariporide to Reduce the Risk of Ischemic Cardiac Events in Patients Undergoing Coronary Artery Bypass Grafting: Results of the EXPEDITION Study.” *Ann Thorac Surg* 85: 1261–70.

Merklinger, Sandra L, Peter L Jones, Eliana C Martinez, and Marlene Rabinovitch. 2005. “Epidermal Growth Factor Receptor Blockade Mediates Smooth Muscle Cell Apoptosis and Improves Survival in Rats with Pulmonary Hypertension.” *Circulation* 112(3): 423–31.

Merklinger, SL., PL. Jones, EC. Martinez, and M. Rabinovitch. 2005. “Epidermal Growth Factor Receptor Blockade Mediates Smooth Muscle Cell Apoptosis and Improves Survival in Rats with Pulmonary Hypertension.” *Circulation* 112(3): 423–31.

Mey, J., RP. Babiuk, R. Clugston, and JJ. Greer. 2003. “Retinal Dehydrogenase-2 Is Inhibited by Compounds That Induce Congenital Diaphragmatic Hernias in Rodents.” *Am J Pathol* 162: 673–79.

Meyrick, B., and L. Reid. 1980. “Ultrastructural Findings in Lung Biopsy Material from Children with Congenital Heart Defects.” *Am. J. Pathol.* 101: 527–37.

Mitani, Y. et al. 2000. “Nitric Oxide Reduces Vascular Smooth Muscle Cell Elastase Activity through cGMP-Mediated Suppression of ERK Phosphorylation and AML1B Nuclear Partitioning.” *FASEB journal* 14(5): 805–14.

Moore, AW. et al. 1998. “YAC Transgenic Analysis Reveals Wilms’ Tumour 1 Gene Activity in the pro- Liferating Coelomic Epithelium, Developing Diaphragm and Limb.” *Mechanisms of Development* 79(1-2): 169–84.

Moore, AW. et al. 1999. “YAC Complementation Shows a Requirement for Wt1 in the Development of Epi- Cardium, Adrenal Gland and throughout Nephrogenesis.” *Development* 126(9): 1845–57.

Nagaoka, T. et al. 2005. “Inhaled Rho Kinase Inhibitors Are Potent and Selective Vasodilators in Rat Pulmonary Hypertension.” *Am J Respir Crit Care Med* 171: 494–99.

Nagase, H., and JF. Woessner. 1999. “Matrix Metalloproteinases.” *J Biol Chem* 274: 21491–94.

Noble, BR. et al. 2007. “Mechanisms of Action of the Congenital Diaphragmatic Hernia-Inducing Teratogen Nitrofen.” *Am J Physiol Lung Cell Mol Physiol* 293(4): L1079–87.

Nogueira-Silva, Cristina et al. 2012. "Local Fetal Lung Renin-Angiotensin System as a Target to Treat Congenital Diaphragmatic Hernia." *Molecular medicine (Cambridge, Mass.)* 18: 231–43.

O'Toole, SJ., MS. Irish, BA. Holm, and PL. Glick. 1996. "Pulmonary Vascular Abnormalities in Congenital Diaphragmatic Hernia." *Department of Surgical Pediatrics* 23(4): 781–94.

Ohuchi, E. et al. 1997. "Membrane Type 1 Matrix Metalloproteinase Digests Interstitial Collagens and Other Extra-Cellular Matrix Macromolecules." *J Biol Chem* 272: 2446–51.

Oka, M. et al. 2007. "Rho Kinase-Mediated Vasoconstriction Is Important in Severe Occlusive Pulmonary Arterial Hypertension in Rats." *Circ Res* 100: 923–29.

Pang, KS. 2003. "Modeling of Intestinal Drug Absorption: Roles of Transporters and Metabolic Enzymes." *Drug metabolism and disposition: the biological fate of chemicals* 31(12): 1507–19.

Pankov, R., and KM. Yamada. 2002. "Fibronectin at a Glance." *Journal of Cell Science* 115: 3861–63.

Penaloza, D. et al. 1964. "The Heart and Pulmonary Circulation in Children at High Altitudes: Physiological, Anatomical, and Clinical Observations." *Pediatrics* 34: 568–82.

Peng, T., and E. Morrisey. 2013. "Development of the Pulmonary Vasculature: Current Understanding and Concepts for the Future." *Pulmonary circulation* 3(1): 176–78.

Pober, BR. 2008. "Genetic Aspects of Human Congenital Diaphragmatic Hernia." *Clin Genet* 74(1): 1–15.

Puri, P., and N. Nakazawa. 2009. "Congenital Diaphragmatic Hernia." In *Pediatric Surgery: Diagnosis and Management.*, eds. P. Puri and M. Hollworth. Springer.

Rabinovitch, M. 2008. "Molecular Pathogenesis of Pulmonary Arterial Hypertension." *The Journal of Clinical Investigation* 118(7): 2372–79.

Rafii, S., and D. Lyden. 2003. "Therapeutic Stem and Progenitor Cell Transplantation for Organ Vascularization and Regeneration." *Nat Med* 9: 702–12.

Ricks, DM. et al. 2008. "Optimized Lentiviral Transduction of Mouse Bone Marrow-Derived Mesenchymal Stem Cells." *Stem cells and development* 17(3): 441–50.

Rotta, A. et al. 1956. "Pulmonary Circulation at Sea Level and at High Altitudes." *J Appl Physiol* 9: 328–36.

Rottier, R., and D. Tibboel. 2005. “Fetal Lung and Diaphragm Development in Congenital Diaphragmatic Hernia.” *Semin Perinatol* 29(2): 86–93.

Rudolph, AM. 1970. “The Changes in the Circulation after Birth. Their Importance in Congenital Heart Disease.” *Circulation* 41(2): 343–59.

Semenza, GL. 2005. “Pulmonary Vascular Responses to Chronic Hypoxia Mediated by Hypoxia-Inducible Factor 1.” *Proc Am Thorac Soc* 2: 68–70.

Shao, D., JE. Park, and SJ. Wort. 2011. “The Role of Endothelin-1 in the Pathogenesis of Pulmonary Arterial Hypertension.” *Pharmacol Res* 63: 504–11.

Shapiro, L., GB. Pott, and AH. Ralston. 2001. “Alpha-1-Antitrypsin Inhibits Human Immunodeficiency Virus Type 1.” *FASEB journal* 15(1): 115–22.

Shaw, L., and O. Wiedow. 2011. “Therapeutic Potential of Human Elafin.” *Biochemical Society transactions* 39(5): 1450–54. http://www.ncbi.nlm.nih.gov/pubmed/21936832 (August 23, 2014).

Shi, Q. et al. 1998. “Evidence for Circulating Bone Marrow-Derived Endothelial Cells.” *Blood* 92: 362–67.

Shimoda, LA. 2010. “Hypoxic Regulation of Ion Channels and Transporters in Pulmonary Vascular Smooth Muscle.” *Adv Exp Med Biol* 661: 221–35.

Shimoda, LA., and J. Polak. 2011. “Theme: Hypoxia. Hypoxia and Ion Channel Function.” *Am J Physiol Cell Physiol* 300(5): C951–67.

Shimoda, LA., JS. Sham, Q. Liu, and JT. Sylvester. 2002. “Acute and Chronic Hypoxic Pulmonary Vasoconstriction: A Central Role for Endothelin-1?” *Respir Physiol Neurobiol* 132: 93–106.

Shipley, JM. et al. 1996. “Metalloelastase Is Required for Macrophage-Mediated Proteolysis and Matrix Invasion in Mice.” *Proc Natl Acad Sci U S A* 93: 3942–46.

Simonneau, G. et al. 2004. “Clinical Classification of Pulmonary Hypertension.” *Journal of the American College of Cardiology* 43(12): 5S – 12S.

Sokol, J. et al. 2002. “Fetal Pulmonary Artery Diameters and Their Association with Lung Hypoplasia and Postnatal Outcome in Congenital Diaphragmatic Hernia.” *Am J Obstet Gynecol* 186(5): 1085–90.

Stenmark, KR. et al. 2009. “Animal Models of Pulmonary Arterial Hypertension: The Hope for Etiological Discovery and Pharmacological Cure.” *Am J Physiol Lung Cell Mol Physiol* 297: L1013–32.

Stenmark, KR., and IF. McMurtry. 2005. "Vascular Remodeling versus Vasoconstriction in Chronic Hypoxic Pulmonary Hypertension: A Time for Reappraisal?" *Circ Res* 97: 95–98.

Stone, LC., and JM. Manson. 1981. "Effects of the Herbicide 2, 4-Dichlorophenyl-P-Nitrophenyl Ether (nitrofen) on Fetal Lung Development in Rats." *Toxicology.* 20(2): 195–207.

Susan, S., B. Hurt, Smith JM., and AW. Hayes. 1983. "NITROFEN: A REVIEW AND PERSPECTIVE." *Toxicology* 29: 1–37.

Takahashi, YI., JE. Smith, and DS. Goodman. 1977. "Vitamin A and Retinol-Binding Protein Metabolism during Fetal Development in the Rat." *Am J Physiol* 233: E263–72.

Taraseviciene-Stewart, L. et al. 2001. "Inhibition of the VEGF Receptor 2 Combined with Chronic Hypoxia Causes Cell Death-Dependent Pulmonary Endothelial Cell Proliferation and Severe Pulmonary Hypertension." *FASEB J* 15: 427–38.

The Neonatal Inhaled Nitric Oxide Study Group (NINOS). 1997. "Inhaled Nitric Oxide and Hypoxic Respiratory Failure in Infants with Congenital Diaphragmatic Hernia." *Pediatrics* 99: 838–45.

Thébaud, B. et al. 1999. "Vitamin A Decreases the Incidence and Severity of Nitrofen-Induced Congenital Diaphragmatic Hernia in Rats." *Am J Physiol* 277(2): L423–29.

Thébaud, B. et al. 2001. "Restoring Effects of Vitamin A on Surfactant Synthesis in Nitrofen-Induced Congenital Diaphragmatic Hernia in Rats." *Am J Respir Crit Care Med* 164: 1083–89.

Thébaud, B., JC. Mercier, and AT. Dinh-Xuan. 1998. "Congenital Diaphragmatic Hernia. A Cause of Persistent Pulmonary Hypertension of the Newborn Which Lacks an Effective Therapy." *Biol Neonate* 74(5): 323–36.

Todorovich-Hunter, L. et al. 1988. "Altered Elastin and Collagen Synthesis Associated with Progressive Pulmonary Hypertension Induced by Monocrotaline: A Biochemical and Ultrastructural Study." *Lab Invest* 58: 184–95.

Tong, QS. et al. 2007. "Nitrofen Suppresses Cell Proliferation and Promotes Mitochondria-Mediated Apoptosis in Type II Pneumocytes." *Acta Pharmacol Sin* 28(5): 672–84.

Torfs, CP., CJ. Curry, TF. Bateson, and LH. Honoré. 1992. "A Population-Based Study of Congenital Diaphragmatic Hernia." *Teratology* 46(6): 555–65.

Tropea, KA. et al. 2012. "Bronchioalveolar Stem Cells Increase after Mesenchymal Stromal Cell Treatment in a Mouse Model of Bronchopulmonary Dysplasia." *Am J Physiol Lung Cell Mol Physiol* 302(9): L829–37.

Tuder, RM. 2009. “Pathology of Pulmonary Arterial Hypertension.” *Semin Respir Crit Care Med* 30: 376–85.

Undem, C., EJ. Rios, J. Maylor, and LA. Shimoda. 2012. “Endothelin-1 Augments Na+/H+ Exchange Activity in Murine Pulmonary Arterial Smooth Muscle Cells via Rho Kinase.” *PLoS One* 7: e46303.

Vincent, SD., and ME. Buckingham. 2010. “How to Make a Heart. The Origin and Regulation of Cardiac Progenitor Cells.” *Current Topics in Developmental Biology* 90(C): 1–41.

Visse, R., and H. Nagase. 2003. “Matrix Metalloproteinases and Tissue Inhibitors of Metalloproteinases: Structure, Function, and Biochemistry.” *Circ Res* 92: 827–39.

Voelkel, NF., and RM. Tuder. 2000. “Hypoxia-Induced Pulmonary Vascular Remodeling: A Model for What Human Disease?” *J Clin Invest* 106: 733–38.

Vogel, C., and EM. Marcotte. 2012. “Insights into the Regulation of Protein Abundance from Proteomic and Transcriptomic Analyses.” *Nature reviews. Genetics* 13(4): 227–32.

Wang, Y. et al. 2013. “Strain-Induced Differentiation of Fetal Type II Epithelial Cells Is Mediated via the Integrin α6β1-ADAM17/tumor Necrosis Factor-A-Converting Enzyme (TACE) Signaling Pathway.” *J Biol Chem* 288(35): 25646–57.

Waszak, P. et al. 2012. “Pre-Conditioning Enhances the Paracrine Effect of Mesenchymal Stem Cells in Preventing Oxygen-Induced Neonatal Lung Injury in Rats.” *Stem Cells Dev* 21: 2789–97.

Weber, SC. et al. 2011. “Isolation and Culture of Fibroblasts, Vascular Smooth Muscle, and Endothelial Cells From the Fetal Rat Ductus Arteriosus.” *Pediatric Research* 70: 236–41.

Weiss, DJ. et al. 2011. “Stem Cells and Cell Therapies in Lung Biology and Lung Diseases.” *Proc Am Thorac Soc.* 8(3): 223–72.

Weiss, DJ. et al. 2013. “A Placebo-Controlled Randomized Trial of Mesenchymal Stem Cells in Chronic Obstructive Pulmonary Disease.” *Chest* 143: 1590–98.

Wells, LJ. 1954. “Development of the Human Diaphragm and Pleural Sacs.” *Contributions to Embryology Carnegie Institute* 35: 107–34.

Wewers, MD., and RG. Crystal. 2013. “Alpha-1 Antitrypsin Augmentation Therapy.” *COPD* 10: 64–67.

Wharton, J. et al. 2005. “Antiproliferative Effects of Phosphodiesterase Type 5 Inhibition in Human Pulmonary Artery Cells.” *Am J Respir Crit Care Med* 172: 105–13.

Whitby, DJ., and MWJ. Ferguson. 1991. “The Extracellular Matrix of Lip Wounds in Fetal, Neonatal and Adult Mice.” *Development* 112: 651–68.

Whitman, EM. et al. 2008. “Endothelin-1 Mediates Hypoxia- Induced Inhibition of Voltage-Gated K+ Channel Expression in Pulmonary Arterial Myocytes.” *Am J Physiol Lung Cell Mol Physiol* 294: L309–18.

Wilson, JG., CB. Roth, and J. Warkany. 1953. “An Analysis of the Syndrome of Malformations Induced by Maternal Vitamin A Deficiency. Effects of Restoration of Vitamin A at Various Times during Gestation.” *Am J Anat* 92: 189–217.

Woessner. 2004. *Handbook of Proteolytic Enzymes*. Second. eds. AJ. Barrett, ND. Rawlings, and J. Fred. London: Elsevier Academic Press.

Woessner, JF. 1998. *The Matrix Metalloproteinase Family.* First. eds. WC. Parks and RP. Mecham. San Diego: Academic Press.

Yamaguchi, J. et al. 2003. “Stromal Cell-Derived Factor-1 Effects on Ex Vivo Expanded Endothelial Progenitor Cell Recruitment for Ischemic Neovascularization.” *Circulation* 107(9): 1322–28.

Yamahara, K. et al. 2008. “Augmentation of Neovascularizaiton in Hindlimb Ischemia by Combined Transplantation of Human Embryonic Stem Cells-Derived Endothelial and Mural Cells.” *PLoS ONE* 3(2): e1666.

Yan, J. et al. 2009. “Recovery from Hind Limb Ischemia Is Less Effective in Type 2 than in Type 1 Diabetic Mice: Roles of Endothelial Nitric Oxide Synthase and Endothelial Progenitor Cells.” *Journal of Vascular Surgery* 50(6): 1412–22.

Yanagisawa, M. et al. 1988. “A Novel Peptide Vasoconstrictor, Endothelin, Is Produced by Vas- Cular Endothelium and Modulates Smooth Muscle Ca2+ Channels.” *J Hypertens Suppl* 6: S188–91.

Yang, J. et al. 2013. “Sildenafil Potentiates Bone Morphogenetic Protein Signaling in Pulmonary Arterial Smooth Muscle Cells and in Experimental Pulmonary Hypertension.” *Arterioscler Thromb Vasc Biol* 33: 34–42.

Yang, X. et al. 2005. “Dysfunctional Smad Signaling Contributes to Abnormal Smooth Muscle Cell Proliferation in Familial Pulmonary Arterial Hypertension.” *Circ Res* 96: 1053–63.

Yang, X. et al. 2007. “BMP4 Induces HO-1 via a Smad-Independent, p38MAPK- Dependent Pathway in Pulmonary Artery Myocytes.” *Am J Respir Cell Mol Biol* 37: 598–605.

Yuan, JX. et al. 1998. “Dysfunctional Voltage-Gated K+ Channels in Pulmonary Artery Smooth Muscle Cells of Patients with Primary Pulmonary Hypertension.” *Circulation* 98: 1400–1406.

Yuan, W. et al. 2003. “A Genetic Model for a Central (septum Transversum) Congenital Diaphragmatic Hernia in Mice Lacking Slit3.” *Proc Natl Acad Sci U S A* 100(9): 5217–22.

Zhao, YD. et al. 2005. “Rescue of Monocrotaline-Induced Pulmonary Arterial Hypertension Using Bone Marrow-Derived Endothelial-like Progenitor Cells: Efficacy of Combined Cell and eNOS Gene Therapy in Established Disease.” *Circulation research* 96(4): 442–50.

Appendix

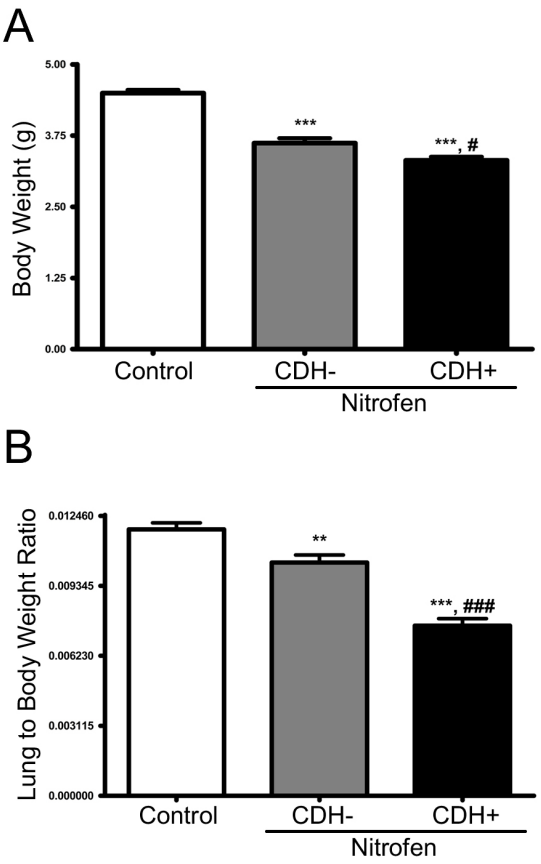

Figure 1. Effect of nitrofen and CDH on body weight and lung hypoplasia. Nitrofen significantly decreased fetal body weight (g) (**A**) and lung weight to body weight ratio (**B**), which were even lower in animals with CDH. (** $P \leq 0.01$ and *** $P \leq 0.001$ compared to Ctl; # $P \leq 0.05$ and ### $P \leq 0.001$ compared to CDH-)

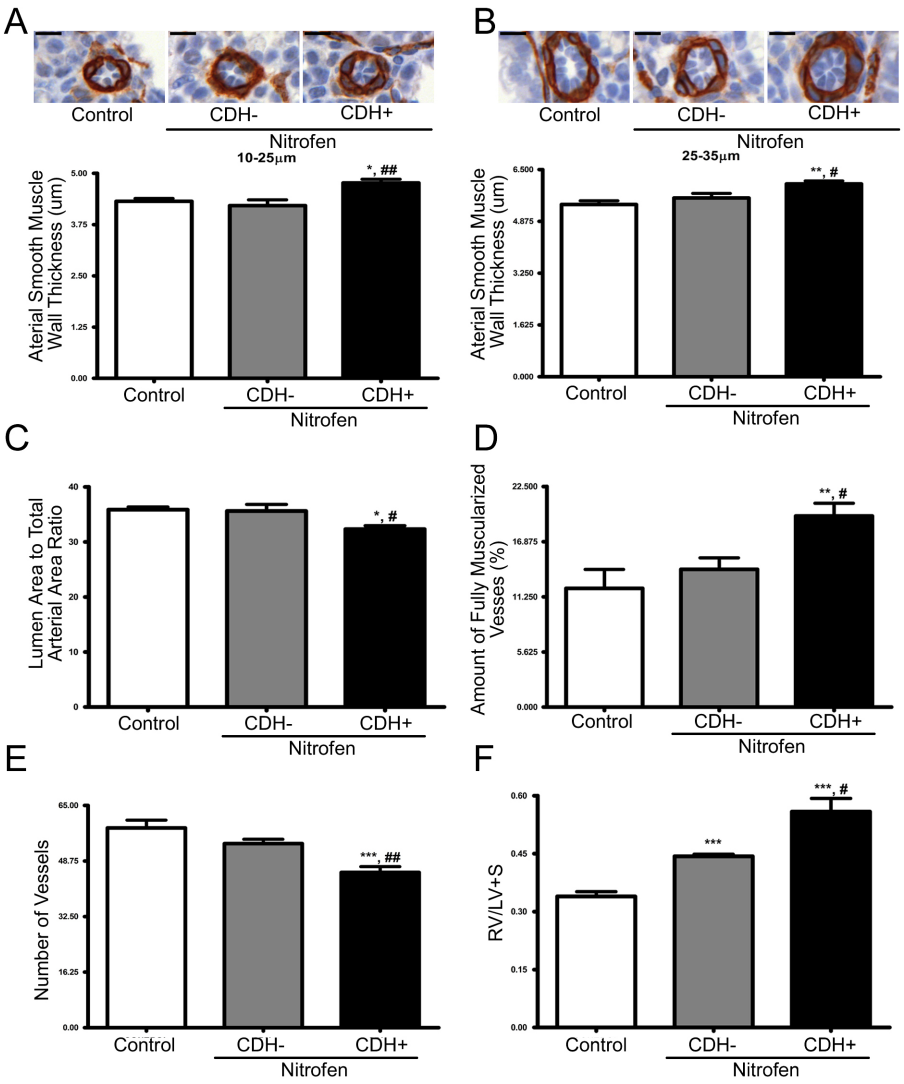

Figure 2. Fetal rats with CDH show features of pulmonary vascular disease. Media wall thickness was increased in PAs of rats with CDH, as shown for PAs of 10-25 μm (**A**) and 25-35 μm (**B**), while the lumen area was decreased (PAs with external diameter of 10-35 μm were measured) (**C**). The percentage of fully muscularized vessels was significantly elevated in fetal rats with CDH (PAs with external diameter of 10-45 μm were measured) (**D**), while the number of vessels was decreased (PAs with external diameter of 10-45 μm were measured) (**E**). The right ventricle (RV) to left ventricle + septum (LV + S) ratio was slightly augmented by exposure of fetal rats to nitrofen, but was further increased in rats with CDH (**F**). Values are shown as means ± SE with N=7 lungs per group **(A-E)**, 10 arteries per lung **(A)**, 15 arteries per lung **(B)**, and 10 hearts per group **(F)**. (* $P \leq 0.05$, ** $P \leq 0.01$, and *** $P \leq 0.001$ compared to Ctl; # $P \leq 0.05$ and ## $P \leq 0.01$ compared to CDH-). Black bar in photomicrographs represents 10um.

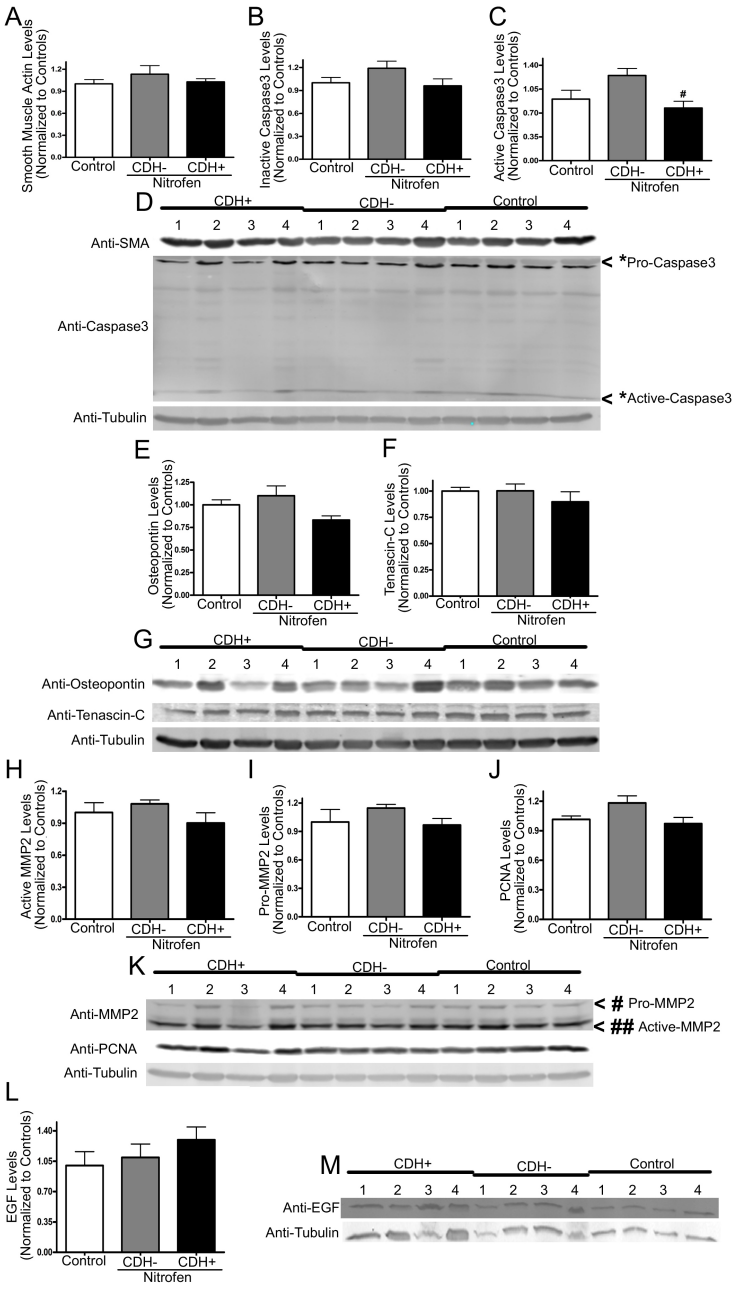

Figure 3. No change in proliferation, apoptosis, smooth muscle actin, MMP2, osteopontin, tenascin-c or EGF levels from whole lung lysates in fetal rats with CDH when compared to controls. (A-C) are graphical representations of **(D)** whereby smooth muscle actin and both (*) inactive and (**) active caspase-3 levels in whole left lung lysates remain unchanged due to the CDH defect. Interestingly active-caspase3 is significantly decreased between CDH- and CDH+ groups. Osteopontin and tenascin-C **(E-F)** levels also are unaffected by CDH. Active MMP2 (##), pro-MMP2 (#), and PCNA **(H-J)** maintain equivalent expression levels independently of CDH defect. EGF **(L)** although slightly elevated in CDH+ lung lysates is not significantly different than either controls or CDH- groups. For all figures n=4 per treatment group as shown. (# $P \leq 0.05$ compared to CDH-).

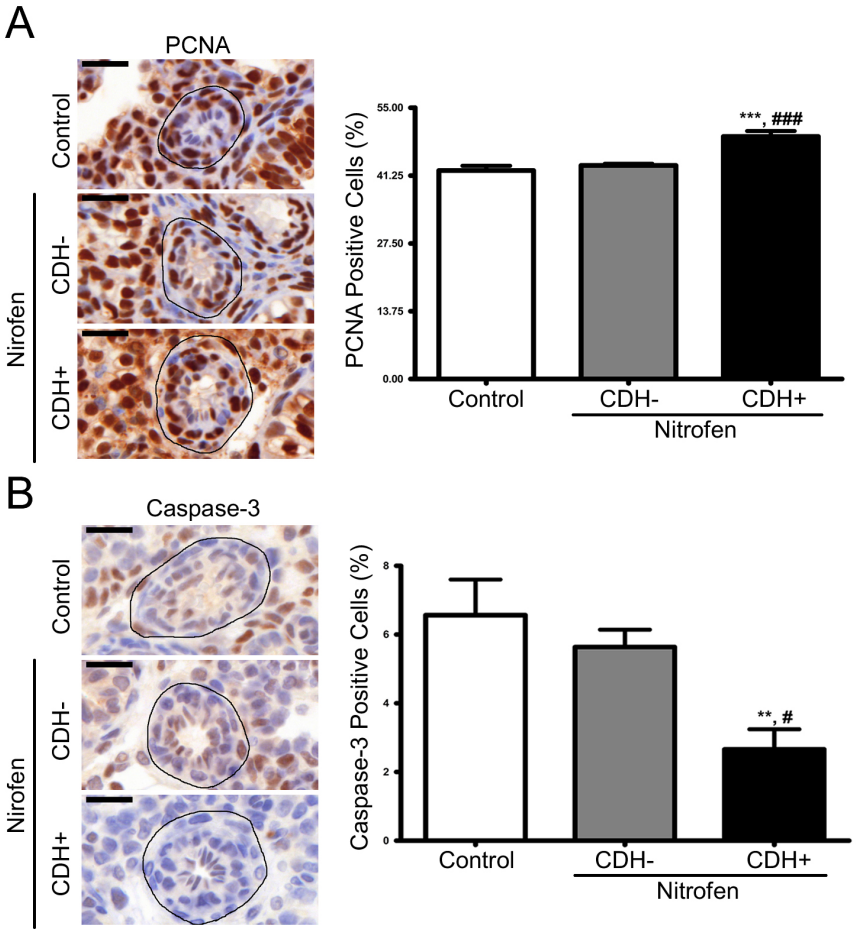

Figure 4. Increased cell proliferation and decreased apoptosis in PAs of fetal rats with CDH. Cell proliferation was assessed by PCNA staining (**A**) and quantified as percentage of PCNA-positive cells in PAs (**B**). Cells were labelled with anti-caspase-3, a marker of apoptosis, (**C**) and the percentage of caspase-3-positive cells in PAs have been determined (**D**). The limits of each PA, as determined by SMA positive staining, are delineated in black in the photomicrographs. Values are shown as means ± SE with N=7 lungs per dose group and 10 arteries per lung. (** $P \leq 0.01$ and *** $P \leq 0.001$ compared to Ctl; # $P \leq 0.05$ and ### $P \leq 0.001$ compared to CDH-). Black bar in photomicrographs represents 10um.

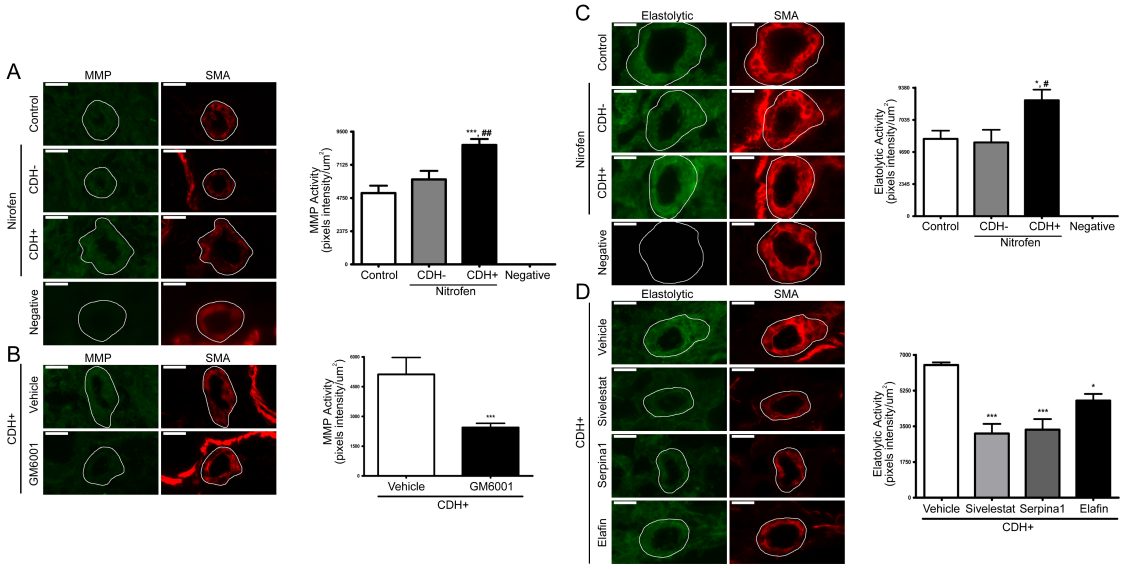

Figure 5. Elastolytic and MMP activities are induced in PAs of fetal rats with CDH. Enzyme activity has been assessed by in situ zymography using a fluorescent substrate in PAs, identified by positive SMA labeling, and quantified as ' Pixels Intensity per μm^2 '. The PAs are encircled with a white line. The MMP activity was significantly increased in PAs of rats with CDH (**A)**. Very low fluorescent signal was detected in the absence of substrate and the CDH-induced MMP activity was significantly reduced by the broad spectrum MMP inhibitor GM6001 **(B)**. The elastolytic activity was also significantly induced in PAs of rats with CDH (**C**). Very low fluorescent signal was detected in the absence of substrate and the CDH-induced elastolytic activity was significantly reduced with both a general, serpina1, and selective, sivelestat, serine elastase inhibitor (**D**). Values are shown as means ± SE with N=7 lungs per dose group and 10 arteries per lung. (* $P \leq 0.05$, ** $P \leq 0.01$, and *** $P \leq 0.001$ compared to Ctl; # $P \leq 0.05$ and ## $P \leq 0.01$ compared to CDH-). White bar in photomicrographs = 20 µm.

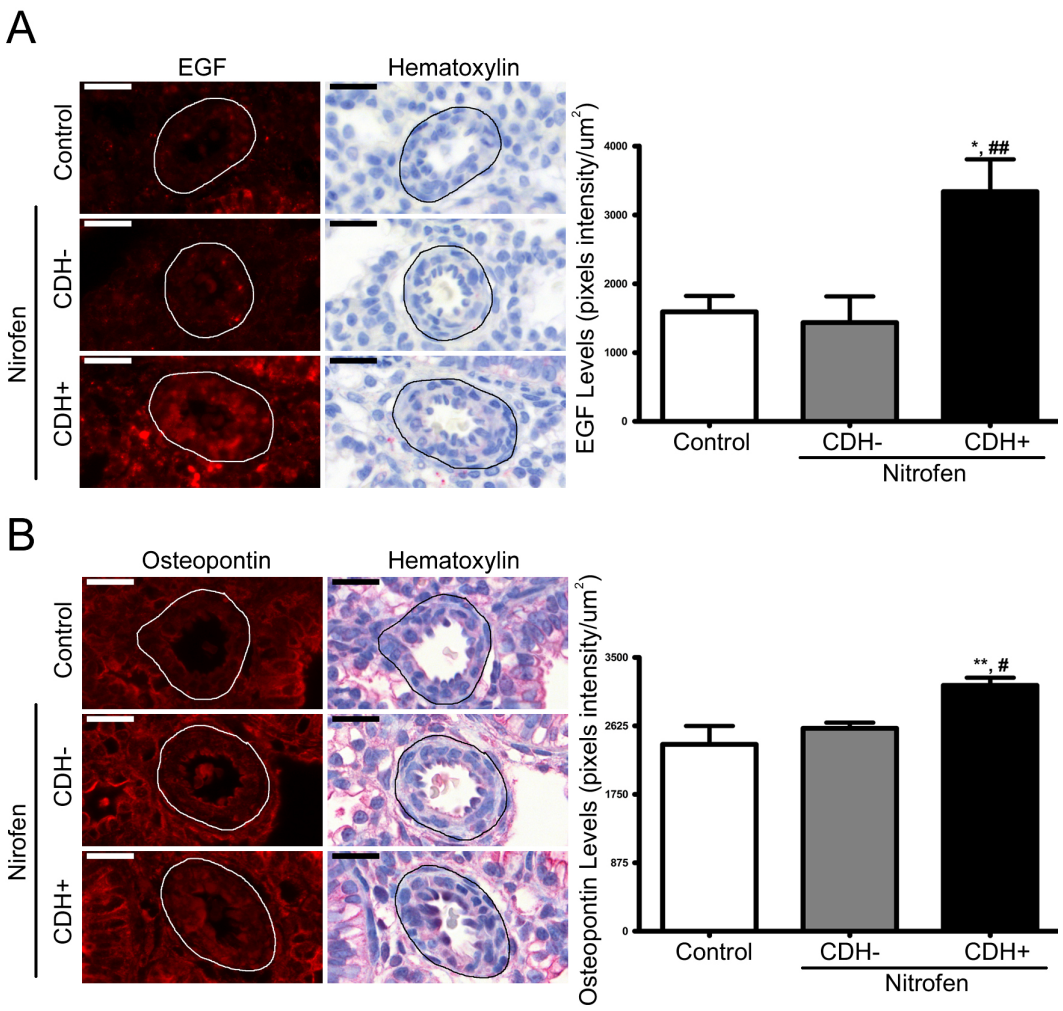

Figure 6. EGF and osteopontin levels are augmented in PAs of fetal rats with CDH. Quantification of EGF **(A)** and osteopontin **(B)** levels in PAs are presented as ' Pixels Intensity per μm^2 '. The limits of each PA, as determined by SMA positive staining, are delineated in black in the photomicrographs. Values are shown as means ± SE with N=7 lungs per dose groups and 10 arteries per lung. (* $P \leq 0.05$ and ** $P \leq 0.01$ compared to Ctl; # $P \leq 0.05$ and ## $P \leq 0.01$ compared to CDH-). Bar = 20 µm.

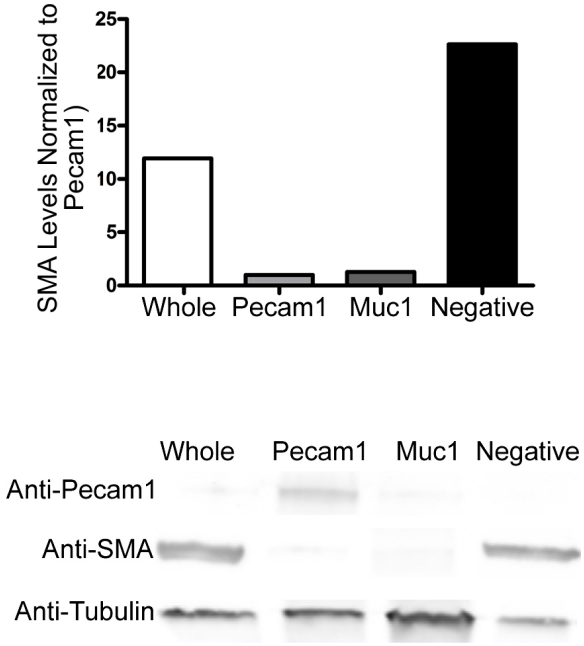

Figure 7. SMC enrichment via magnetic cell sorting was accomplished by removing endothelial cells, epithelial cells, alveolar cells, and pneumocytes using PECAM-1 and MUC1 antibodies. SMA levels were quantified via Western blotting and normalized to tubulin. SMA was absent in PECAM-1 and MUC1 positive cell fractions and was doubled in the negative fraction when compared to whole lung lysates indicating an enrichment of SMCs.

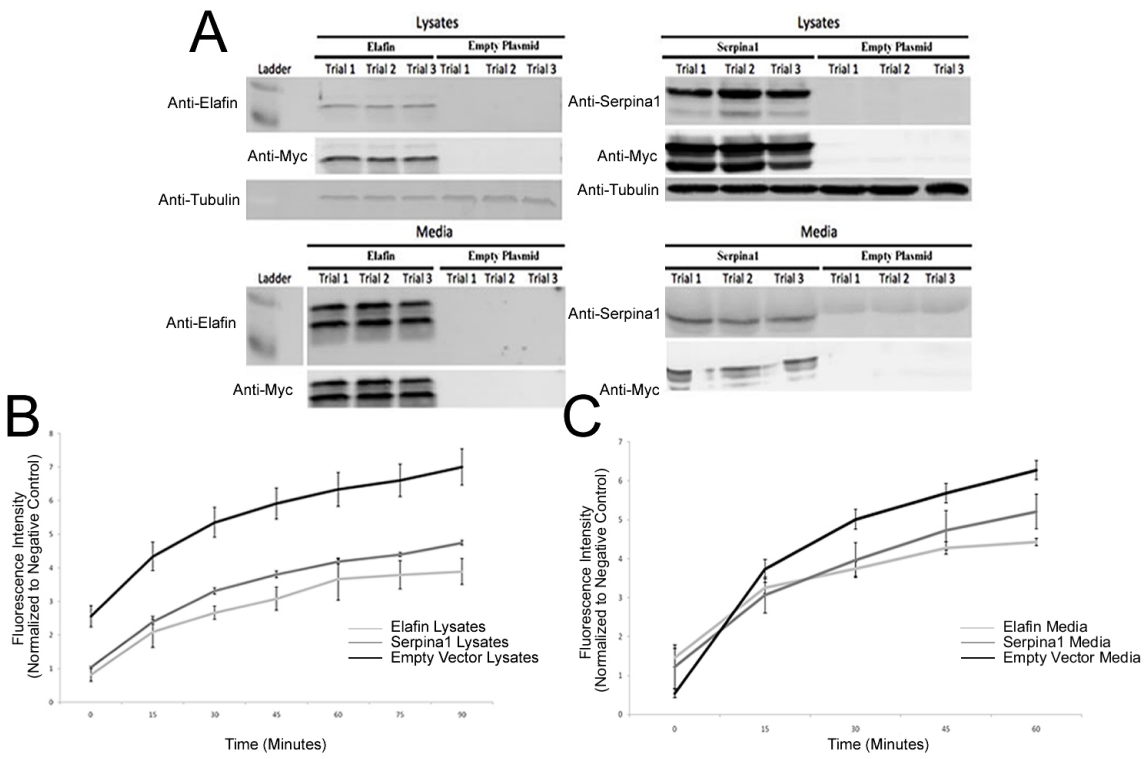

Figure 8. Myc-DDK tagged elafin and serpina1 protein serine elastase inhibitors are secreted from transfected HEK293T cells and inhibit elastase activity. Western blots showing elafin and serpina1 transfected HEK293T lysates and conditioned media compared to HEK293T cells transfected with an empty GFP expressing plasmid done in triplicate **(A)**. Lysates **(B)** and media **(C)** from elafin and serpina1 transfected cells inhibit porcine pancreatic elastase activity as compared to cells transfected with an empty GFP plasmid. The elastase assays were performed with an n=3. (* $P \leq 0.05$)

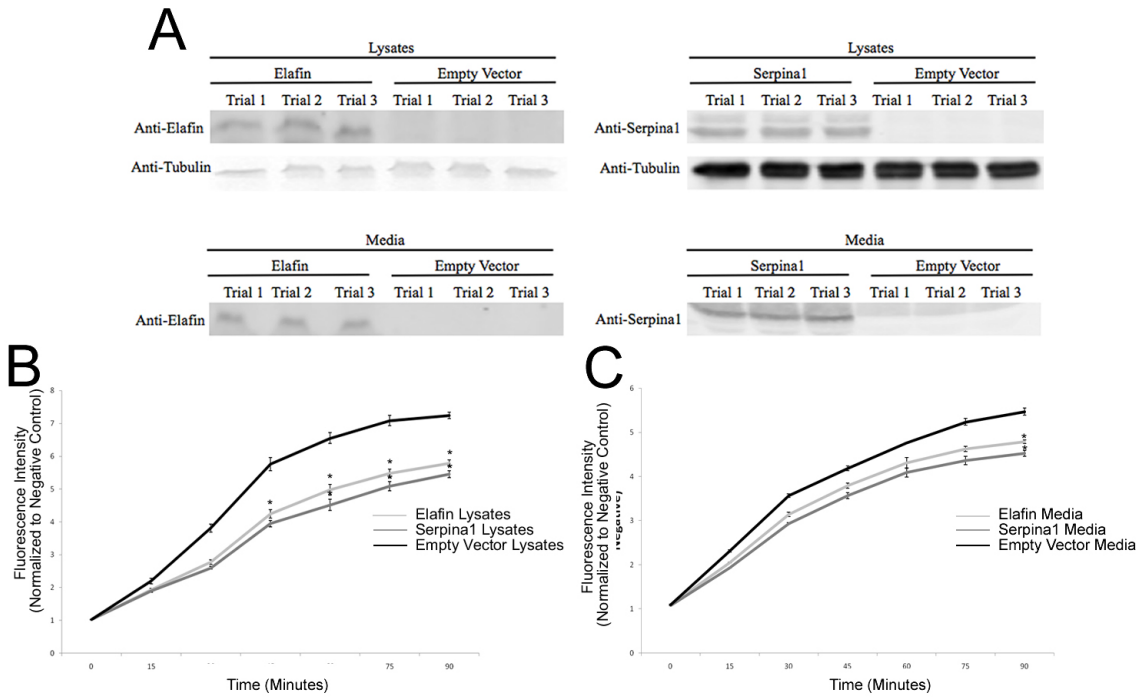

Figure 9. Lentiviral particles containing elafin and serpina1 genes are able to create stable HEK293T cells expressing elafin and serpina1 elastase inhibitors. A western blot showing elafin and serpina1 infected HEK293T lysates and conditioned media compared to HEK293T cells infected with an empty GFP expressing lentiviral plasmid done in triplicate **(A)**. Lysates **(B)** and media **(C)** from elafin and serpina1 infected cells inhibit elastase activity as compared to cells transfected with an empty GFP plasmid. The elastase assays were performed with an n=3. (* $P \leq 0.05$)

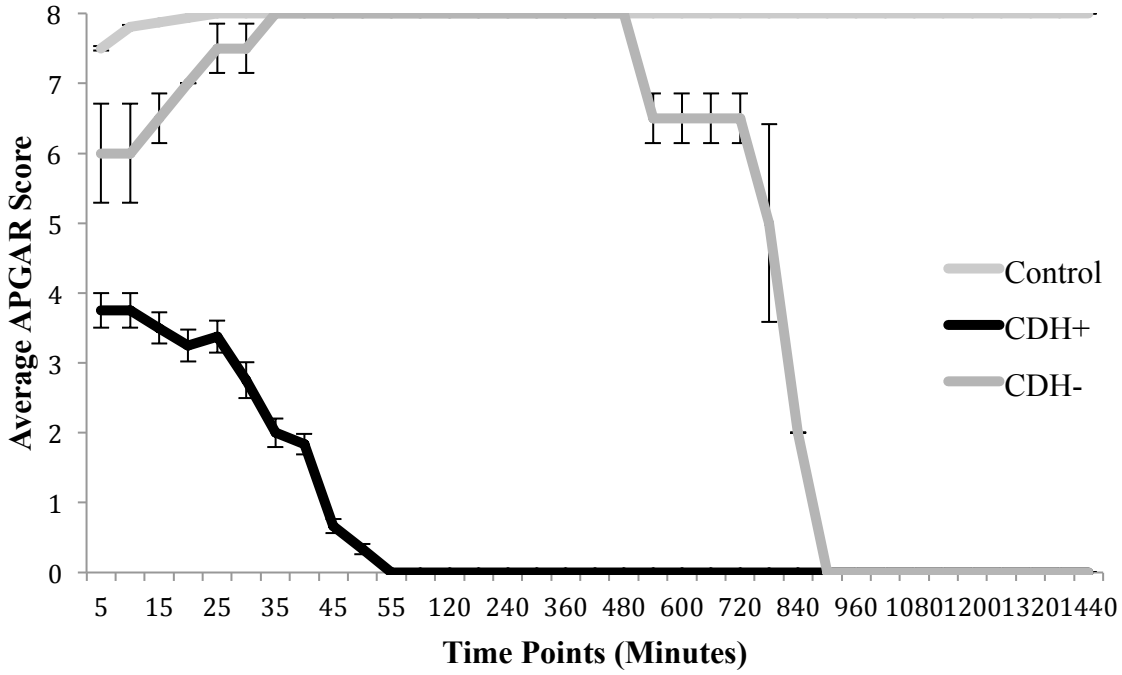

Figure 10. Nitrofen dosed rat pups with or without CDH all die within 1 or 15 hours respectively. Maternal rats were gavage fed 100mg of nitrofen in olive oil (CDH+ and CDH-) or olive oil (Control). Pups were monitored immediately after birth and scored every 5 minutes for the first hour and ever hour for the proceeding 23 hours. APGAR scores were calculated by assigning 2, 1, or 0 to spontaneous motor movement, degree of cyanosis, breathing, and responsive motor movement where 2 is normal and 0 is poor. Data represents n=16 for controls, n=8 for CDH+ and n=7 for CDH-.